Molecular Biology of the Cell
Vol. 9, 3475–3492, December 1998

Functional Characterization of a Nup159p-containing Nuclear Pore Subcomplex

Naïma Belgareh,*† Christine Snay-Hodge,†‡ Fabien Pasteau,* Suzanne Dagher,‡§ Charles N. Cole,‡ and Valérie Doye*‖

*Centre National de la Recherche Scientifique, UMR144, Institut Curie, 75 248 Paris cedex 05, France; and ‡Department of Biochemistry, Dartmouth Medical School, Hanover, New Hampshire 03755

Submitted April 3, 1998; Accepted September 16, 1998
Monitoring Editor: Pamela A. Silver

Nup159p/Rat7p is an essential FG repeat–containing nucleoporin localized at the cytoplasmic face of the nuclear pore complex (NPC) and involved in poly(A)$^+$ RNA export and NPC distribution. A detailed structural–functional analysis of this nucleoporin previously demonstrated that Nup159p is anchored within the NPC through its essential carboxyl-terminal domain. In this study, we demonstrate that Nup159p specifically interacts through this domain with both Nsp1p and Nup82p. Further analysis of the interactions within the Nup159p/Nsp1p/Nup82p subcomplex using the *nup82Δ108* mutant strain revealed that a deletion within the carboxyl-terminal domain of Nup82p prevents its interaction with Nsp1p but does not affect the interaction between Nup159p and Nsp1p. Moreover, immunofluorescence analysis demonstrated that Nup159p is delocalized from the NPC in *nup82Δ108* cells grown at 37°C, a temperature at which the Nup82Δ108p mutant protein becomes degraded. This suggests that Nup82p may act as a docking site for a core complex composed of the repeat-containing nucleoporins Nup159p and Nsp1p. In vivo transport assays further revealed that *nup82Δ108* and *nup159-1/rat7-1* mutant strains have little if any defect in nuclear protein import and protein export. Together our data suggest that the poly(A)$^+$ RNA export defect previously observed in *nup82* mutant cells might be due to the loss from the NPCs of the repeat-containing nucleoporin Nup159p.

INTRODUCTION

Information about the mechanisms by which macromolecules are transported across the nuclear envelope has grown significantly in recent years (for reviews, see Corbett and Silver, 1997; Nigg, 1997; Ohno *et al.*, 1998). This bidirectional transport occurs through nuclear pore complexes (NPCs),[1] which are supramolecular protein assemblies spanning the nuclear envelope and estimated to be composed of ~50 proteins, called nucleoporins (NUPs) (Rout and Blobel, 1993; Matunis and Blobel, 1996). Despite this complexity, it is now expected that all yeast nucleoporins will soon be identified, whereas progress identifying vertebrate nucleoporins is steady, albeit slower (Doye and Hurt, 1997).

On a structural level, a distinguishing feature of ~15 nucleoporins identified in yeast or vertebrates are their repeat domains, consisting of iterative FG, FXFG, or GLFG sequences with variable spacer regions between repeats. In vitro binding studies, in conjunction with specific coimmunoprecipitations in vivo, strongly suggest that these FG-containing domains represent binding sites for a family of soluble transport receptors that belong to the importin β/karyopherin β family (reviewed in Wente *et al.*, 1996; Corbett and Silver, 1997; Ohno *et al.*, 1998; see

† These authors contributed equally to this study.
§ Present address: Department of Biology, University of California at San Diego, La Jolla, CA 92037.
‖ Corresponding author. E-mail address: vdoye@curie.fr.
[1] Abbreviations used: CCD, charge-coupled device; GFP, green fluorescent protein; HA, hemagglutinin; hnRNP, heterogeneous nuclear ribonucleoprotein; HRP, horseradish peroxidase; NES, nuclear export signal; NLS, nuclear localization signal; NPC, nuclear pore complex; NUP, nucleoporin; ProtA, protein A; ts, temperature-sensitive; wt, wild-type.

also Fornerod *et al.*, 1997; Iovine and Wente, 1997; Neville *et al.*, 1997; Pemberton *et al.*, 1997; Rosenblum *et al.*, 1997; Yaseen and Blobel, 1997). In addition, other nucleoporins have been demonstrated to contain binding sites for the small GTPase Ran, an effector of nuclear transport (for reviews, see Corbett and Silver, 1997; Nigg, 1997).

Although we are beginning to understand the interactions between transport factors and individual nucleoporins, the next level of transport research will be directed at understanding these individual nucleoporins in the context of the overall architecture of the NPC. Understanding how nucleoporins assemble into functional subcomplexes and how these subcomplexes are organized within the NPC will help explain how the architectural layout of the NPC contributes to the docking and translocation processes. To that end, most of the identified vertebrate nucleoporins have been localized by immunoelectron microscopy to various NPC substructures, including the central plug, the cytoplasmic filaments, and the filamentous basket-like structure located at the nucleoplasmic face of the NPC (reviewed in Panté and Aebi, 1996; also see Hu *et al.*, 1996; Cordes *et al.*, 1997). In yeast, however, so far only Nup159p and Nup188p have been localized by immunoelectron microscopy to specific NPC substructures (Kraemer *et al.*, 1995; Nehrbass et al., 1996).

Biochemical approaches have revealed that heptad repeats favoring α-helical coiled-coil structures are one of the major structural motifs through which nucleoporins bind to each other. Among the yeast nucleoporins that contain coiled-coil domains, Nsp1p, Nup49p, and Nup57p constitute a subcomplex to which Nic96p is more loosely associated (Grandi *et al.*, 1993, 1995b). A distinct fraction of Nsp1p was also found to be associated with the carboxyl-terminal coiled-coil domain of Nup82p, an essential nucleoporin required for poly(A)$^+$ RNA export (Grandi *et al.*, 1995a; Hurwitz and Blobel, 1995). Another yeast NPC subcomplex identified includes Nup120p, Nup84p, Nup85p, the in vivo–cleaved carboxyl-terminal half of Nup145p, Seh1p, and a fraction of Sec13p (Siniossoglou *et al.*, 1996; Teixeira *et al.*, 1997). In contrast to the other well-characterized yeast and vertebrate NPC subcomplexes, none of these nucleoporins contains putative coiled-coil domains. Disruption of the genes encoding Nup84p, Nup85p, or Nup120p or deletion of the carboxyl-terminal domain of Nup145p caused a temperature-sensitive (ts) phenotype associated with defects in poly(A)$^+$ RNA export at the restrictive temperature as well as a constitutive clustering of NPCs (Wente and Blobel, 1994; Aitchison *et al.*, 1995a; Heath *et al.*, 1995; Goldstein *et al.*, 1996; Siniossoglou *et al.*, 1996; Teixeira *et al.*, 1997).

A few other yeast nucleoporin mutants have been shown to affect both poly(A)$^+$ RNA export and NPC distribution (for review, see Doye and Hurt, 1997). Among them is the *rat7-1/nup159-1* allele, identified in a screen for mRNA export mutants (Gorsch *et al.*, 1995). The *RAT7/NUP159* gene (hereafter referred to as *NUP159*) encodes an essential FG repeat-containing nucleoporin localized at the cytoplasmic face of the NPC (Gorsch *et al.*, 1995; Kraemer *et al.*, 1995). A specific feature of the *nup159-1* mutant is that the NPC clustering phenotype is not constitutive, because shifting *nup159-1* mutant cells to 37°C restores nearly wild-type NPC distribution (Gorsch *et al.*, 1995). A detailed structural–functional analysis of Nup159p recently revealed that the two predicted coiled-coil regions located near the carboxyl-terminal domain of Nup159p are the only essential domains of the protein and suggested that this carboxyl-terminal domain is required to anchor Nup159p within the NPC (Del Priore *et al.*, 1998).

In this study, we demonstrate that Nup159p associates with both Nup82p and Nsp1p. Within this nuclear pore subcomplex, interactions are mediated by coiled-coil domains present in the three nucleoporins. Biochemical and immunofluorescence studies performed with *nup82* and *nup159* mutant strains further revealed that the carboxyl-terminal domain of Nup82p anchors Nup159p at the cytoplasmic face of the NPC, whereas the carboxyl-terminal domain of Nup159p is required for the stability of the Nup159p/Nsp1p/Nup82p subcomplex. In agreement with these results, in vivo studies revealed that carboxyl-terminal truncation of Nup159p and Nup82p led to similar defects in NPC distribution and nucleocytoplasmic transport.

MATERIALS AND METHODS

Plasmid and Strain Construction

The yeast plasmids and strains used in this study are listed in Tables 1 and 2. DNA manipulations including restriction endonuclease analyses, fill-in reactions with Klenow fragment, and ligations were performed essentially as described (Maniatis *et al.*, 1982). Microbiological techniques, including yeast growth on minimal or YPD medium, plasmid transformation, and plasmid recovery, were performed as described (Wimmer *et al.*, 1992a), except that minimal SD medium was supplemented either with a 0.1 g/l concentration of each amino acid and nucleic acid base component (obtained from Sigma Chemical, St. Louis, MO) except those used for selection, or in the case of medium lacking uracil and/or tryptophan, by 5 g/l casamino acids (Difco, Detroit, MI), 0.1 g/l adenine, and 0.1 g/l uracil or tryptophan.

To construct the *ProtA-C-NSP1*, *ProtA-C-nsp1-ala6*, *GFP-C-NSP1*, and *GFP-C-nsp1-ala6* strains, the pSB32-ProtA-C-NSP1, pSB32-ProtA-C-nsp1-ala6, pSB32-GFP-C-NSP1, and pSB32-GFP-C-nsp1-ala6 plasmids, respectively, were introduced into the *R24* strain that carries a disrupted chromosomal *NSP1* gene and is complemented by the wild-type *NSP1* allele on an *ADE3/URA3*-containing plasmid (Wimmer *et al.*, 1992a). Colonies were selected on SD-Leu plates, and the transformants were plated on 5-fluoro orotic acid–containing medium to select for cells that have lost the pCH1122-URA3-ADE3-NSP1 plasmid. As expected, the *ProtA-C-nsp1-ala6* and *GFP-C-nsp1-ala6* strains displayed a ts phenotype.

Table 1. Plasmids used in this study

Plasmid		Comments	Reference
pSB32-ProtA-C-NSP1	ARS1, CEN4, LEU2	4 IgG binding domains of the proteinA fused to the carboxyl-terminal domain of NSP1 and expressed under the control of the authentic *NSP1* promotor.	Grandi *et al.*, 1993
pSB32-ProtA-C-nsp1-ala6	ARS1, CEN4, LEU2	Same construct as the pSB32-ProtA-C-NSP1 plasmid, except that within the carboxyl-terminal domain of Nsp1p, 6 positively charged amino acids were replaced by alanine residues.	Grandi *et al.*, 1993
pRS316-ProtA-C-NSP1	ARSH4, CEN6, URA3	The *Bam*H1 fragment from plasmid pSB32-ProtA-NSP1 was subcloned into the *Bam*H1 site of the pRS316 plasmid (Sikorski and Hieter, 1989).	This study
pSB32-GFP-C-NSP1	ARS1, CEN4, LEU2	A *Sac*II fragment obtained by PCR and encoding the GFP S65T/V163A variant (Kahana and Silver, 1996) was used to replace the *Sac*II fragment corresponding to the ProtA domain of the pSB32-ProtA-C-NSP1 plasmid.	This study
pSB32-GFP-C-nsp1-ala6	ARS1, CEN4, LEU2	A *Sac*II fragment obtained by PCR and encoding the GFP S65T/V163A variant (Kahana and Silver, 1996) was used to replace the *Sac*II fragment corresponding to the ProtA domain of the pSB32-ProtA-C-nsp1-ala6 plasmid.	This study
pUN100-ProtA-NUP49	ARS1, CEN4, LEU2	Containing 4 IgG binding domains of *S. aureus* protein A in fusion with the complete *NUP49* gene.	Wimmer *et al.*, 1992a
pUN100-GFP-NUP49	ARS1, CEN4, LEU2	Containing the GFP (S65T, V163A) fused to the amino terminus of *NUP49* and with the authentic *NUP49* promotor.	Belgareh and Doye, 1997
pFL38-GFP-NUP49	ARS, CEN, URA3	The 4.26-kb *Sac*I–*Bam*HI fragment of GFP-NUP49 from the pUN100-GFP-NUP49 plasmid was inserted into pFL38.	Constructed by S. Camier (CEA, Saclay, France)
pUN100-ProtA-NUP82	ARS1, CEN4, LEU2	Containing the fusion gene between IgG binding domains of protein A joined to the amino-terminal end of Nup82p and expressed under the *NOP1* promoter.	Grandi *et al.*, 1995a
pRS316-ProtA-NUP82	ARSH4, CEN6, URA3	The *Bam*HI–*Hin*dIII fragment from pUN100-ProtA-NUP82 was subcloned into the pRS316 plasmid (Sikorski and Hieter, 1989).	This study
pUN100-ProtA-N-nup82	ARS1, CEN4, LEU2	An internal *Pvu*II–*Nco*I blunt-ended deletion within the pUN100-ProtA-NUP82 plasmid was used to generate a stop codon at amino acid 460 of Nup82p.	This study
pRS315-ProtA-C-nup82	ARSH4, CEN6, LEU2	The *Bam*HI–*Eco*RI blunt-ended fragment from the pUN100-ProtA-NOP1 plasmid (Berges *et al.*, 1994) containing the 2 IgG binding domains of ProtA under the control of the *NOP1* promotor was fused in frame to the *Pvu*II–*Hin*dIII fragment from the pUN100-ProtA-NUP82 plasmid that encodes the last 251 amino acids of Nup82p, and inserted in the pRS315 vector (Sikorski and Hieter, 1989) opened at its *Bam*HI–*Hin*dIII sites.	This study
pUN100-GFP-NUP82	ARS1, CEN4, LEU2	A *Sph*I–*Sac*I fragment obtained by PCR and encoding the GFP S65T/V163A variant (Kahana and Silver, 1996) was used to replace the *Sph*I–*Sac*I fragment corresponding to the ProtA domain of the pUN100-ProtA-NUP82 plasmid.	This study
pRS316-NUP82	ARSH4, CEN6, URA3	A *Sac*I–*Hin*dIII fragment containing the entire NUP82 gene and cloned into vector pRS316 (Sikorski and Hieter, 1989).	Grandi *et al.*, 1995a
pNUP82-wt	ARSH4, CEN6, LEU2	A PCR product of *NUP82,* fused in frame with two epitopes of the influenza HA protein, and inserted into pRS315.	Hurwitz and Blobel, 1995
pRS314-NUP82-HA	ARSH4, CEN6, TRP1	A *Hin*dIII blunt-ended fragment from the pNUP82-wt plasmid (Hurwitz and Blobel, 1995) encoding the HA-epitope-tagged Nup82p was inserted into the *Sma*I site of the pRS314 plasmid (Sikorski and Hieter, 1989).	This study
pNUP82-Δ108	2μ, LEU2	A PCR product missing the last 324 nucleotides of *NUP82,* fused in frame with two epitopes of the influenza hemagglutinin protein and inserted into a modified Yeplac181 plasmid	Hurwitz and Blobel, 1995
pBM3405	2μ, URA3	Mig1-GFP-β-galactosidase fusion in a 2μ, URA3 vector	De Vit *et al.*, 1997
pKW430	2μ, URA3	Contains the NLS-GFP2-NES fusion expressed under the control of the ADH1 promotor in the pRS424 plasmid	Stade *et al.*, 1997

Table 2. Yeast strains

Strain	Genotype	Reference
BJ2168	*Mat**a** leu2 trp1 ura3-52 pep4-3 pre1-407 prb1-1122*	Aris and Blobel, 1988
FY86	*Mat**a** his3Δ200 ura3-52 leu2Δ1*	Gorsch *et al*., 1995
VDPY121 *(nup159-ΔN)*	*Mat**a** his3Δ200 ura3-52 leu2Δ1 rat7::HIS3* (pVDP16-LEU2–rat7-ΔN)	Del Priore *et al*., 1998
VDPY122 *(nup159-C)*	*Mat**a** his3Δ200 ura3-52 leu2Δ1 rat7::HIS3* (pVDP17-LEU2-rat7-C)	Del Priore *et al*., 1998
LGY101 *(nup159-1)*	*Mat**a** his3Δ200 ura3-52 leu2Δ1 rat7-1^{ts}*	Gorsch *et al*., 1995
NUP82-WT	*Mat**a** his3Δ200 leu2-3,112 lys2-801 trp1-1 ura3-52 nup82::HIS3* (pNUP82-WT-LEU2)	Hurwitz and Blobel, 1995
nup82-Δ87	*Mat**a** his3Δ200 leu2-3,112 lys2-801 trp1-1 ura3-52 nup82::HIS3* (pNUP82-Δ87-LEU2)	Hurwitz and Blobel, 1995
nup82-Δ108	*Mat**a** his3Δ200 leu2-3,112 lys2-801 trp1-1 ura3-52 nup82::HIS3* (pNUP82-Δ108-LEU2)	Hurwitz and Blobel, 1995
NUP82 shuffle	*Mat**a** ade2 trp1 leu2 ura3 his3 nup82::HIS3* (pRS316-URA3-NUP82)	Grandi *et al*., 1995a
GFP-NUP82 (YV201)	*Mat**a** ade2 trp1 leu2 ura3 his3 nup82::HIS3* (pUN100-LEU2-GFP-NUP82)	This study
GFP-NUP82/nup159-1 (YV384)	*Mat? trp? leu2 ura3 his3 nup82::HIS3 rat7-1^{ts}* (pUN100-LEU2-GFP-NUP82)	This study
xpo1-1	*Mat? ade2-1 ura3-1 his3-11,15 trp1-1 leu2-3,112 can1-100 xpo1::LEU2* (pKW457=pRS313-HIS3-xpo1-1)	Stade *et al*., 1997
nsp1-ala6	*Mat**a** ade2 trp1 leu2 ura3 nsp1-ala6::HIS3*	Wimmer *et al*., 1992b
R24	*Mat**a** ade2 ade3 leu2 ura3 trp1 HIS3::nsp1* (pCH1122-URA3-ADE3-NSP1)	Wimmer *et al*., 1992a
ProtA-C-NSP1	*Mat**a** ade2 ade3 leu2 ura3 trp1 HIS3::nsp1* (pSB32-ProtA-C-NSP1)	This study
ProtA-C-nsp1-ala6	*Mat**a** ade2 ade3 leu2 ura3 trp1 HIS3::nsp1* (pSB32-ProtA-C-nsp1-ala6)	This study
GFP-C-NSP1	*Mat**a** ade2 ade3 leu2 ura3 trp1 HIS3::nsp1* (pSB32-GFP-C-NSP1)	This study
GFP-C-nsp1-ala6	*Mat**a** ade2 ade3 leu2 ura3 trp1 HIS3::nsp1* (pSB32-GFP-C-nsp1-ala6)	This study

Similarly, to construct the *GFP-NUP82* strain, the pUN100-GFP-NUP82 plasmid was introduced into the "*NUP82* shuffle" strain (Grandi *et al*., 1995a). Colonies were selected on SD-Leu plates, and the transformants were plated on 5-fluoro orotic acid–containing medium to select for cells that have lost the *URA3*-containing pRS316-NUP82 plasmid.

To combine the *nup159-1* allele and the GFP-NUP82 construct, the *GFP-NUP82* strain was mated with the *LGY101* strain that carries an integrated *nup159-1* allele. Diploids growing on SD-leu-trp medium were sporulated. Haploid progeny was selected that were his$^+$, leu$^+$, and temperature sensitive.

Preparation of Whole-Cell Extract

Whole-cell extracts were prepared by resuspending freshly harvested cells from a 20-ml culture (OD_{600}, 1.0) in 0.5 ml of lysis buffer (PBS, 2 mM EDTA, 2.5 mM PMSF, 2.5 mg/ml protease inhibitors). Glass beads (0.4 g) were added, and the samples were incubated during 0.5 h at 4°C with continuous vortexing. The extracts were centrifuged, and the supernatants were diluted with 2× Laemmli buffer (1× Laemli buffer: 62.5 mM Tris, pH 6.8, 10% glycerol, 3% SDS, 5% β-mercaptoethanol) and boiled for 3 min. Aliquots corresponding to 20 μg proteins (as measured by the dye-binding assay of Bradford, 1976) were analyzed on 8% SDS-polyacrylamide gels.

Purification of Protein A Fusion Proteins by IgG-Sepharose Chromatography

Affinity purification of protein A (ProtA)–tagged nucleoporins by IgG-Sepharose chromatography from whole-cell lysates under nondenaturing conditions was performed essentially as described (Grandi *et al*., 1993; Siniossoglou *et al*., 1996). Briefly, yeast cells expressing the various protein A–tagged nucleoporins were grown to an OD_{600} of 1.0 and converted into spheroplasts by treatment with Zymolyase (Seikagaku America, Rockville, MD). Spheroplasts were lysed in 30 ml of lysis buffer (0.5% Triton X-100, 20 mM Tris, pH 8.0, 150 mM KCl, 5 mM $MgCl_2$, and a mixture of protease inhibitors) by performing 10 strokes with a Dounce homogenizer. The lysed spheroplasts were centrifuged for 10 min at 40,000 × *g*, and the supernatant was loaded onto a 3-mm-diameter column packed with IgG-Sepharose (Pharmacia, Uppsala, Sweden) and equilibrated with lysis buffer. The column was then successively washed with 10–15 ml lysis buffer and 5 ml 5 mM NH_4OAc (pH 5.0). The bound proteins were eluted with 1.5 ml 0.5 M acetic acid/NH_4OAc (pH 3.4), lyophilized, and resuspended in Laemmli buffer. For the experiments presented in Figure 2B, the originally published lysis buffer (2% Triton X-100, 20 mM NaCl, 0.2 mM $MgCl_2$, 20 mM Tris-HCl, pH 8.0) and washing conditions (Grandi *et al*., 1993) were used and gave similar results similar to those obtained with the above-mentioned protocol.

Western Blot Analysis

Proteins were separated on 8% SDS-polyacrylamide gels and transferred to nitrocellulose (Schleicher & Schuell, Keene, NH). Membranes were blocked in Tris-buffered saline plus 0.1% Tween 20 and 5% nonfat milk powder. To decrease nonspecific cross-reactivity of the antibodies with the protein A moiety of the fusion proteins, 10% human serum was added during the various incubation steps. Antibodies were diluted in Tris-buffered saline plus 0.1% Tween 20 and 5% nonfat milk powder at the following dilutions: IgGs coupled to horseradish peroxidase (HRP; Dakopatts, Glostrup, Denmark), 1:5000; rat7#4, raised in guinea pig against the repeat region of Nup159p (Gorsch *et al*., 1995), 1:10,000; rat7#5, raised in rabbit against the carboxyl domain of Nup159p (Del Priore *et al*., 1998), 1:5000; anti-Nsp1p, directed at the repeated domains of Nsp1p (Nehrbass *et al*., 1990), 1:2000; anti-hemagglutinin (HA), 12CA5 mAb (Babco, Richmond, CA), 1:2500; anti-Nic96p, raised in rabbit against the amino-terminal domain of Nic96p (Grandi *et al*., 1995b), 1:500; and anti-Nup133p directed at the amino-terminal domain of Nup133p (Belgareh and Doye, 1997), 1:250. The secondary antibodies were goat anti-mouse or anti-rabbit IgGs coupled to HRP (Jackson ImmunoResearch), 1:5000, and goat anti-guinea pig IgG coupled to alkaline phosphatase (Sigma), 1:1000.

Fluorescence and Immunofluorescence Experiments

Indirect immunofluorescence was performed as described previously (Gorsch *et al*., 1995). Briefly, cells were grown overnight to

early log phase, shifted for 3 h to 37°C, fixed with 3.7% formaldehyde (Fisher Scientific, Pittsburgh, PA), washed, and converted to spheroplasts by using 300 mg/ml Zymolyase 100T. Cells were incubated overnight at 4°C with the rat7#4 antibody (Gorsch *et al.*, 1995) diluted 1:3000. Cells were washed and then incubated with an FITC-conjugated anti-guinea pig IgG secondary antibody (Vector Laboratories, Burlingame, CA) at a dilution of 1:250 and viewed and photographed with a Zeiss (Thornwood, NY) Axiphot microscope equipped with a charge-coupled device (CCD) camera.

Protein export assays were performed as described (Stade *et al.*, 1997) using the NLS-GFP2-NES (nuclear localization signal-2 green fluorescent protein molecules-nuclear export signal) reporter protein. Cells were grown to early log phase, shifted to 37°C for 2 h, collected by brief centrifugation, and resuspend in 1 ml medium. Four microliters of cells were spotted onto coverslips coated with 1% polyethylenimine and viewed as above.

To visualize NPC distribution in living cells, the strains were transformed with the pFL38-GFP-NUP49 plasmid which encodes a form of Nup49p tagged with GFP (Belgareh and Doye, 1997). To visualize GFP-Nup82p, cells were grown in SD medium lacking uracil to midlog phase at the indicated temperature and shifted for 2 h to 37°C. To inhibit protein synthesis, cultures were treated with either 10 or 30 μg cycloheximide per ml, added 5 min before shifting to 37°C.

For the in vivo analysis of nuclear protein import, wild-type or nucleoporin mutant cells expressing the Mig1p-GFP-LacZ reporter (De Vit *et al.*, 1997) were grown overnight at 25°C in SD-uracil medium. This primary culture was used to inoculate secondary cultures of SGly-uracil medium (5% glycerol, 6.7 g/l yeast nitrogen base without amino acids, 5% casamino acids, 0.1 mg/l adenine and tryptophan). Cells were then grown at 25°C to an OD_{600} of ~0.5 and either kept at 25°C or shifted for 2 h to 37°C. One milliliter of cell suspension was transferred to a prewarmed Eppendorf (Madison, WI) tube, briefly centrifuged, resuspended in 100 μl SGly-uracil medium, and kept at the appropriate temperature. At this stage, 10 μl of a 20% glucose solution was added to induce the nuclear import of the Mig1p-GFP-LacZ reporter (defining this time as t = 0). Five microliters of cells were rapidly placed between a slide and a coverslip and observed by fluorescence microscopy using the FITC channel. A given field was recorded at various times after the addition of glucose (routinely t = 1, 3, 5, and 8 min) using a CCD camera. Alternatively, cells were kept at 25 or 37°C for 5 or 10 min after glucose addition, and independent fields were recorded.

For in vivo fluorescence analysis, 5–10 μl of cells expressing the appropriate GFP-fusion protein were placed on a microscope slide and covered with a coverslip. Images were obtained by using a cooled CCD camera (Hamamatsu Photonics, Hamamatsu City, Japan) on a microscope (Leica, Deerfield, IL) equipped with the following filter set: excitation, 450–490 nm; dichroic, 510 nm; emission, 515–560 nm (filter L4, Leica), a 100-W mercury arc lamp, and a 100×, numerical aperture 1.4 objective lens. Identical exposure conditions were used for all comparable images, and composites were prepared using Adobe (Mountain View, CA) Photoshop with identical brightness and contrast optimization for all comparable images within a figure.

Electron Microscopy Experiments

Cells were examined by electron microscopy as previously described (Byers and Goetsch, 1975; Wright and Rine, 1989; Goldstein *et al.*, 1996), except that cells were incubated for 4 h at 16°C. Thin sections of 90 nm were cut on a MT5000 ultramicrotome (Dupont Sorvall, Norwalk, CT), poststained in 2% uranyl acetate and Reynold's lead citrate, and then examined and photographed using a Jeol (Tokyo, Japan) 100CX electron microscope at 80 kV.

RESULTS

Nup159p Is Part of the Nsp1p- and Nup82p-containing NPC Subcomplex

Most of the yeast nucleoporins that contain heptad repeats have been shown to be part of one of two distinct nuclear pore subcomplexes: the Nsp1p/Nup49p/Nup57p/Nic96p subcomplex and the Nsp1p/Nup82p subcomplex (Grandi *et al.*, 1993, 1995a,b). Because the identification of yeast nucleoporins is close to completion (Doye and Hurt, 1997), we were interested in determining with which nucleoporins the heptad repeat containing nucleoporin Nup159p interacted. We began by determining whether Nup159p might associate with either of these two subcomplexes. Because Nup159p is highly sensitive to proteolysis (Gorsch *et al.*, 1995; Kraemer *et al.*, 1995), affinity chromatography under nondenaturing conditions was carried out using whole-cell lysates obtained from protease-deficient BJ2168 strains (Figure 1, A and B) expressing ProtA-Nup49p, ProtA-C-Nsp1p, or ProtA-Nup82p (the ProtA tag refers to two or four IgG binding sequences from the *Staphylococcus aureus* protein A; ProtA-C-Nsp1p only contains the essential carboxyl-terminal domain of Nsp1p; see Table 1). The purified fractions, isolated by IgG-Sepharose chromatography, were probed with IgG coupled to HRP to detect the fusion proteins (α-ProtA) or with a polyclonal antibody directed against the central FG repeat–containing domain of Nup159p (Figure 1A). Full-length Nup159p migrating with an apparent molecular mass of 205 kDa (Gorsch *et al.*, 1995; Kraemer *et al.*, 1995), as well as faster-migrating bands corresponding to Nup159p breakdown products, were detected with the anti-Nup159p antibody in both the ProtA-C-Nsp1p and ProtA-Nup82p eluates but not in the ProtA-Nup49p fraction. These results thus demonstrate that Nup159p interacts, directly or indirectly, with both Nup82p and the carboxyl-terminal domain of Nsp1p.

To determine the relative abundance of Nsp1p and Nup159p in the ProtA-Nup82p complex, affinity-purified fractions obtained from the protease-deficient BJ2168 strain expressing ProtA-Nup82p (or ProtA-Nup49p used as a control) were stained with Coomassie blue. In this experiment, Nup159p and Nsp1p were especially well preserved from proteolysis, which enabled us to detect these two proteins by Coomassie blue staining (Figure 1B). Under those conditions, no other major purifying proteins could be detected in the ProtA-Nup82p eluate.

To quantify the fraction of Nup159p that is associated to the Nsp1p/Nup82p subcomplex, affinity purification of ProtA-C-Nsp1p expressed in an *NSP1*-disrupted strain was performed, and aliquots of the load (soluble fraction from the whole-cell lysates), of the unbound (flow-through) and of the bound and subsequently eluted fractions were coincidentally analyzed. As shown in Figure 1C, this revealed that a major

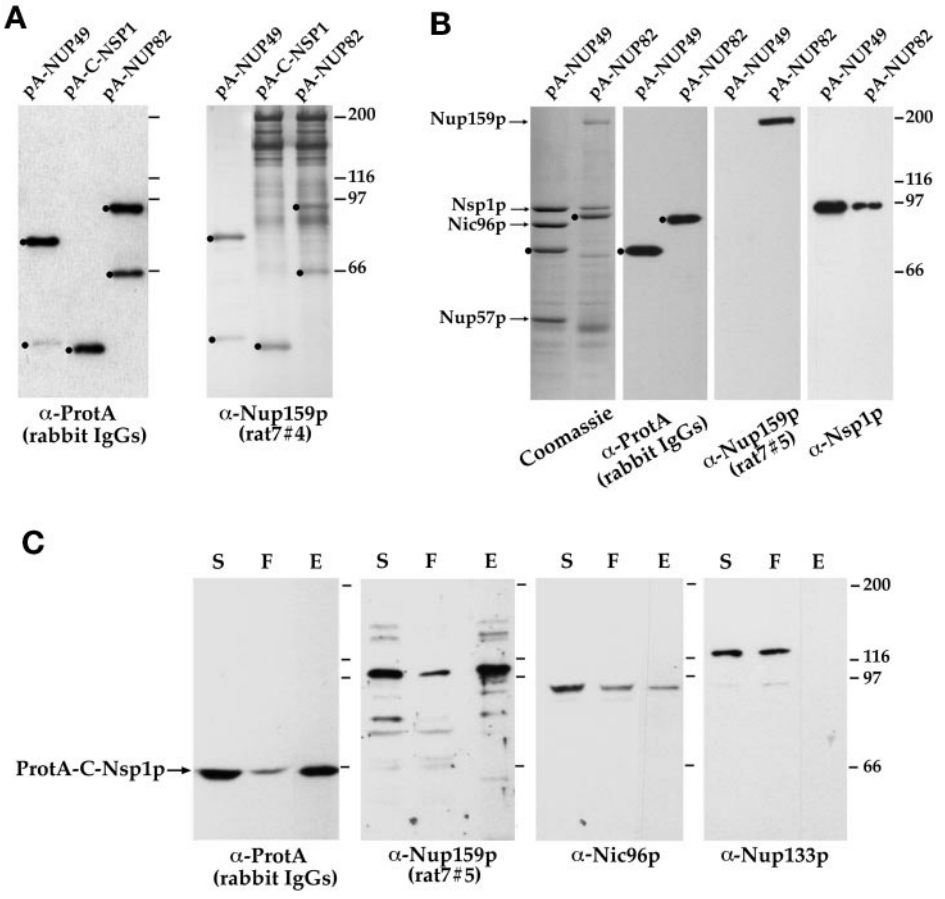

Figure 1. Nup159p interacts with Nup82p and Nsp1p. (A and B) ProtA-Nup49p, ProtA-Nup82p, and ProtA-C-Nsp1p expressed in the protease-deficient BJ2168 strain were affinity purified by chromatography on IgG-Sepharose as described in MATERIALS AND METHODS. (A) Purified fractions from the ProtA-Nup49p, ProtA-C-Nsp1p, and ProtA-Nup82p affinity columns were analyzed by immunoblotting after SDS-PAGE, using IgG coupled to HRP to visualize the ProtA-fusion proteins (α-ProtA) and an anti-Nup159p antibody directed against the repeat motifs of Nup159p (rat7#4, see MATERIALS AND METHODS). The positions of the ProtA fusion proteins (dots) are indicated. Note that the rat7#4 antibody also cross-reacts with ProtA chimeras. (B) Eluted fractions from the ProtA-Nup49p and ProtA-Nup82p affinity columns were analyzed by SDS-PAGE followed by Coomassie blue staining or by Western blotting using IgG coupled to HRP to visualize the ProtA constructs, an antibody directed against the carboxyl-terminal domain of Nup159p (rat7#5), and an anti-Nsp1p antibody directed against the repeat domain of Nsp1p. Coomassie blue staining reveals Nsp1p, Nic96p, and Nup57p in the ProtA-Nup49p–purified fraction, whereas Nsp1p and Nup159p copurify with the ProtA-Nup82p fusion protein. The positions of Nup159p, Nsp1p, Nic96p, Nup57p (arrows), and the ProtA fusion proteins (dots) are indicated. (C) Affinity purification of ProtA-C-Nsp1p expressed in an *NSP1*-disrupted strain. Equivalent amounts of the load (soluble fraction from the whole-cell lysates [S]), of the unbound (flow-through [F]), and of the bound and subsequently eluted (E) fractions were analyzed by Western blotting. IgGs coupled to HRP were used to detect ProtA-C-Nsp1p, the rat7#5 antibody to visualize Nup159p, and antibodies directed against Nic96p and Nup133p were used as controls. Note that the *NSP1*-disrupted strain is not protease deficient, leading to a substantial degradation of Nup159p with a major degradation product migrating at ~100 kDa.

fraction of Nup159p (equivalent to the fraction of ProtA-C-Nsp1p that is bound and subsequently eluted from the IgG-Sepharose column) can be copurified with ProtA-C-Nsp1p under our lysis conditions (the *NSP1*-disrupted strain is not protease deficient, leading to a substantial degradation of Nup159p). In contrast, <50% of Nic96p copurified with ProtA-C-Nsp1p under these conditions. Nic96p being one of the most abundant nucleoporins (Aitchison *et al.*, 1995b), this result might reflect the fact that, unlike Nup159p, which mainly interacts with the Nsp1p-Nup82p complex, Nic96p might be associated with several NPC subcomplexes. These results, together with the presence of equivalent amounts of Nup159p in both ProtA-Nup82p and ProtA-C-Nsp1p eluates (Figure 1A) and the previously reported interaction between Nsp1p and Nup82p (Grandi *et al.*, 1995a), therefore demonstrate that these three proteins are the major components of a distinct nuclear pore subcomplex.

Mutations within the Carboxyl-terminal Domain of Nsp1p Affect Its Interaction with Both the Nup82p/Nup159p- and the Nic96p-containing Subcomplexes

Previous studies, based on the affinity purification of ProtA-C-nsp1-ala6p expressed in a wild-type *NSP1* (*wtNSP1*) background (Grandi *et al.*, 1993) indicated that the *ProtA-C-nsp1-ala6* mutant allele was not able to interact with Nic96p but was still able to interact with an 80-kDa species comigrating with the 80-kDa band seen with intact ProtA-C-Nsp1p (and subsequently identified as Nup82p; Grandi *et al.*, 1995a). Unexpectedly, we found that when ProtA-C-nsp1-ala6p was expressed in an *nsp1*-disrupted strain, both Nup159p and Nic96p copurified as efficiently with ProtA-C-nsp1-ala6p as with ProtA-C-Nsp1p (Figure 2A). When similar studies were performed in a wtNsp1p background (as originally published), the use of HA-tagged Nup82p revealed that the interac-

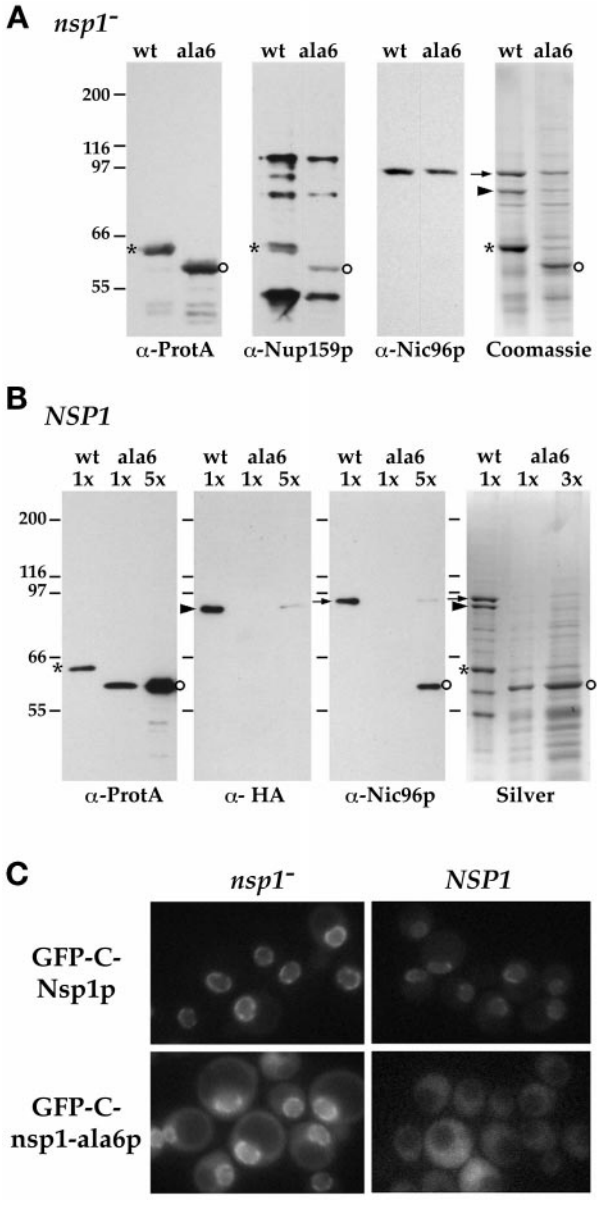

Figure 2. In the presence of wild-type Nsp1p, Nsp1-ala6p no longer interacts with Nup82p and Nic96p and is not targeted to the NPC. (A) Yeast cells with a disrupted chromosomal copy of *NSP1* and complemented by ProtA-C-Nsp1p (wt) or ProtA-C-nsp1-ala6p (ala6) were grown at 24°C. Whole-cell lysates from these two strains were affinity purified by IgG-Sepharose chromatography. The affinity-purified fractions were analyzed by Western blotting for the presence of ProtA-C-Nsp1p (asterisks) or ProtA-C-nsp1-ala6p (open circles), Nup159p (using the rat7#5 antibody), and Nic96p, or by Coomassie blue staining. In this *nsp1*$^-$ background, both ProtA-C-Nsp1p and ProtA-C-nsp1-ala6p were able to interact with Nup159p and Nic96p. Nic96p (arrow) and Nup82p (arrowhead) could also be detected by Coomassie blue staining of the two eluates. Note that in this strain background, Nup159p was degraded during the purification procedure and was therefore hardly detectable by Coomassie blue staining. (B) Whole-cell lysates from *NUP82-HA* cells carrying a wild-type chromosomal copy of *NSP1* and expressing ProtA-C-Nsp1p (wt) or ProtA-C-nsp1-ala6p (ala6) were affinity purified by IgG-Sepharose chromatography as described in MATERIALS AND METHODS. The eluates were analyzed by silver staining (Silver) or by Western blot using an anti-IgG coupled to HRP to detect ProtA-C-Nsp1p (asterisks) or ProtA-C-nsp1-ala6p (open circles), an anti-HA antibody to detect Nup82-HAp (arrrowhead), or an antiNic96p (arrow). In the presence of wild-type Nsp1p, the interaction between ProtA-C-nsp1-ala6p and both Nup82-HAp and Nic96p was inhibited (a very faint band was detectable only when a fivefold excess of the ProtA-C-nsp1-ala6 eluate was loaded). (C) The *GFP-C-NSP1* and *GFP-C-nsp1-ala6* fusion genes were expressed in an *NSP1*-disrupted strain (*nsp1*$^-$) and in a wild-type strain (*NSP1*). The GFP-C-Nsp1p and GFP-C-nsp1-ala6p signals were observed by fluorescence microscopy in living cells grown at 24°C as described in MATERIALS AND METHODS.

tion between ProtA-C-nsp1-ala6p and both Nic96p and Nup82p was impaired (Figure 2B). Accordingly, the 80-kDa species comigrating with the 80-kDa band seen with ProtA-C-Nsp1p (Grandi *et al.*, 1995a) is not Nup82p but most likely corresponds to a nonspecific interacting protein. In agreement with these biochemical data, we observed that unlike GFP-C-Nsp1p, GFP-nsp1-ala6p is not efficiently targeted to the NPC in wild-type cells (i.e., when wtNsp1p is present) and only becomes targeted in the absence of Nsp1p (Figure 2C). These results therefore demonstrate that the interaction between *nsp1-ala6* and both Nic96p and Nup82p is compromised in the presence of competing Nsp1p. Accordingly, identical or overlapping domain(s) within the heptad repeat sequence of Nsp1p might be involved in the interaction in the context of both the Nsp1p/Nup159p/Nup82p and the Nsp1p/Nup49p/Nup57p/Nic96p NPC subcomplexes.

A Deletion within the Heptad Repeat–containing Carboxyl-terminal Domain of Nup82p Destabilizes Its Interaction with the Nsp1p/Nup159p Complex

The heptad repeat-containing carboxyl-terminal domain of Nup82p has been shown previously to interact with the essential carboxyl-terminal domain of Nsp1p that also contains heptad repeats (Grandi *et al.*, 1995a). To examine whether this domain of Nup82p is also involved in the interaction with Nup159p, the ProtA-N-nup82p and ProtA-C-nup82p constructs, containing the amino- and carboxyl-terminal domains of Nup82p, respectively (see Table 1), and the ProtA-Nup82p construct were introduced into the BJ2168 protease-deficient strain, and affinity chromatography was performed on whole-cell extracts. Equal amounts of eluates were tested for the presence of Nup159p, and, as control, for the presence of Nsp1p (Figure 3A). Nup159p was found to interact with the carboxyl-terminal domain of Nup82p (although to a lower extent compared with Nsp1p), whereas no interaction was detected with the amino-terminal construct. This result therefore suggests that the heptad repeat–containing carboxyl-terminal domain of Nup82p is in-

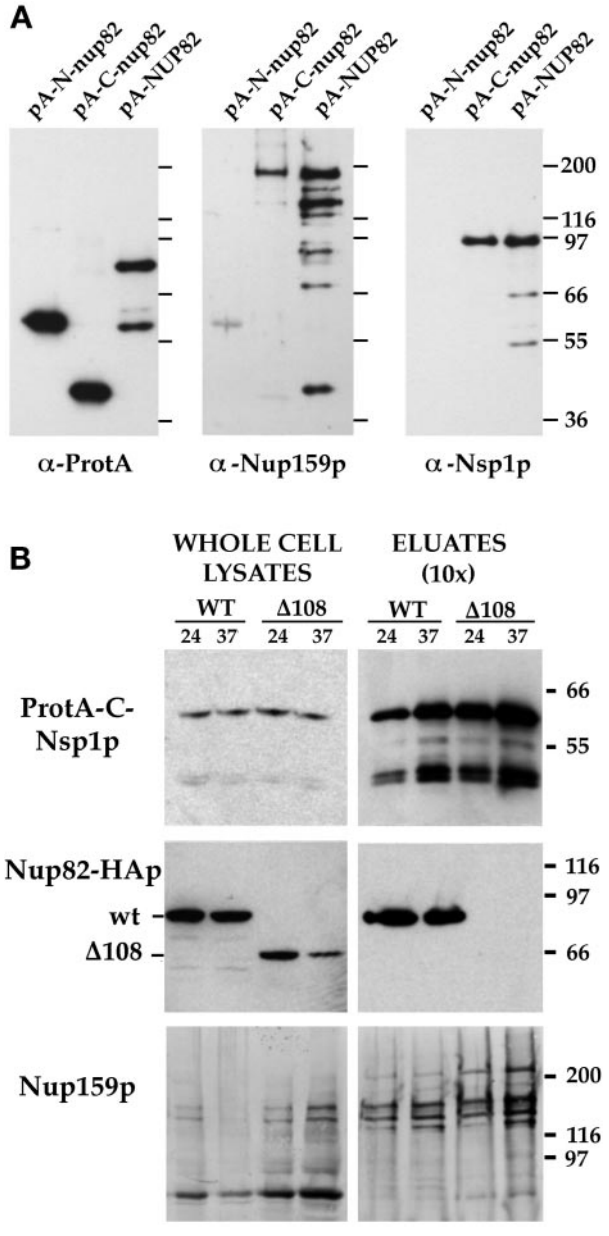

Figure 3. Nsp1p and Nup159p form a core complex independent of interaction with the carboxyl-terminal domain of Nup82p. (A) Affinity purification by IgG-Sepharose chromatography of ProtA-N-nup82p, ProtA-C-nup82p, and ProtA-Nup82p expressed in strains derived from BJ2168. The purified fractions were analyzed by Western blotting using IgG coupled to HRP to detect the ProtA fusions, an anti-Nup159p antibody directed against the carboxyl-terminal domain of Nup159p (rat7#5), and an antibody directed against the repeat domain of Nsp1p. (B) Whole-cell lysates from *NUP82* (WT) and *nup82-Δ108* (Δ108) strains transformed with the pRS316-ProtA-C-Nsp1p plasmid and maintained at 24°C or shifted to 37°C for 3 h were affinity purified by IgG-Sepharose chromatography. Whole-cell lysates and affinity-purified fractions (eluates, 10-fold equivalent) were analyzed by Western blotting for the presence of ProtA-C-Nsp1p using an anti-IgG coupled to HRP, for the presence of Nup82-HAp and Nup82-Δ108-HAp with a monoclonal antibody directed against the HA epitope, and for the presence of Nup159p with the rat7#4 antibody. Although Nup82-Δ108-HAp does not interact with ProtA-C-Nsp1p at either 24 or 37°C, Nup159p still copurifies with ProtA-C-Nsp1p in the *nup82Δ108* strain. Note that the *NUP82-wt* and *nup82Δ108* strains are not protease deficient, leading to a substantial degradation of Nup159p. The shorter degradation product of Nup159p did not copurify with ProtA-C-Nsp1p.

volved in the interaction with both Nsp1p and Nup159p. However, as previously reported (Grandi *et al*., 1995a), neither ProtA-N-nup82p nor ProtA-C-nup82p is able to complement the lethal phenotype of a *nup82*-disrupted strain. Furthermore, analysis of the localization of GFP-tagged N-nup82p or C-nup82p did not reveal a specific targeting of either of these two constructs in a wild-type strain (Belgareh and Doye, unpublished results). Accordingly, the experiments presented in Figure 3A could only be conducted in the presence of wtNup82p, which might compete with ProtA-N-nup82p or ProtA-C-nup82p (as observed above in the case of ProtA-C-nsp1-ala6p).

To further characterize the role of the coiled-coil domain of Nup82p in the assembly of the Nsp1p/Nup159p/Nup82p complex, we therefore introduced the ProtA-C-Nsp1p construct into the *NUP82-wt* and the *nup82Δ108* strains, producing either full-length HA epitope-tagged Nup82p or a mutant form of Nup82p deleted for its last 108 amino acids and thus lacking the second half of its putative coiled-coil domain (Hurwitz and Blobel, 1995). Cells expressing Nup82Δ108p on a high-copy plasmid as the only form of Nup82p were temperature sensitive for growth (Hurwitz and Blobel, 1995), whereas cells in which the mutant allele was present on a centromeric plasmid grew very poorly, even at permissive temperature (our unpublished results). As previously reported (Hurwitz and Blobel, 1995), immunoblotting using the anti-HA monoclonal antibody revealed a decrease in the total amount of Nup82Δ108p when *nup82Δ108* cells were shifted for 3 h to 37°C (Figure 3B), whereas wild-type Nup82p remains stable. Affinity purification on IgG-Sepharose was carried out using whole-cell lysates from *NUP82-wt* or *nup82Δ108* strains expressing ProtA-C-Nsp1p and grown at permissive temperature (24°C) or shifted to 37°C for 3 h. Western blot analysis revealed that, unlike wild-type Nup82p, the Nup82Δ108p protein did not copurify with ProtA-C-Nsp1p, even when cells were grown at permissive temperature (Figure 3B). Similar results were obtained with the *nup82Δ87* strain (our unpublished results), even though this strain does not display a ts phenotype (Hurwitz and Blobel, 1995). This indicates that a deletion within the carboxyl-terminal domain of Nup82p destabilizes its interaction with Nsp1p (i.e., this interaction is no longer stable under our lysis conditions). Interestingly, however, the anti-Nup159p antibody revealed the presence of equivalent amount

of Nup159p in the ProtA-C-Nsp1p eluates from both *NUP82-wt*, and *nup82Δ108* strains (Figure 3B). This indicates that the presence of Nup82p is not required for the interaction between Nsp1p and Nup159p.

The Carboxyl-terminal Domain of Nup159p Is Required for the Stability of the Nup159p/Nsp1p/Nup82p Complex

To specify the domains of Nup159p involved in the interaction with Nsp1p and Nup82p, the ProtA-C-NSP1 and ProtA-NUP82 constructs were introduced into the *nup159-ΔN* mutant, which produces a form of Nup159p lacking its amino terminus (amino acids 1–456), and the *nup159-C* mutant, in which only the carboxyl-terminal third of Nup159p, containing the essential heptad repeat, remains (Del Priore *et al.*, 1998). IgG-Sepharose chromatography was performed, and equal amounts of eluates were tested for the presence of Nup159p by immunoblotting using an antibody to the carboxyl-terminal portion of Nup159p. Both the Nup159-ΔNp and Nup159-Cp truncated proteins were detected in interactions with ProtA-C-Nsp1p (Figure 4A) and ProtA-Nup82p (Figure 4B), indicating that the heptad repeat-containing carboxyl-terminal domain of Nup159p is sufficient for its interaction with both Nsp1p and Nup82p.

We subsequently analyzed the behavior of the Nup159p/Nsp1p/Nup82p subcomplex in the *nup159-1* mutant strain, which produces a protein truncated for its last 96 amino acids and which is degraded after a shift to 37°C (Gorsch *et al.*, 1995; Del Priore *et al.*, 1998; see Figure 4C). Western blot analysis of ProtA-C-Nsp1p copurifying proteins in *nup159-1* mutant cells grown at 24°C revealed that the Nup159-1p mutant protein no longer interacts with ProtA-C-Nsp1p (Figure 4D). Under those lysis conditions, the interaction between ProtA-C-Nsp1p and Nup82p was also inhibited. This suggests that the heptad repeat–containing domain of Nup159p establishes a link between Nsp1p and Nup82p, or that Nup82p can only interact with a preassembled Nsp1p/Nup159p subcomplex. In contrast, the amount of copurifying Nic96p, used as control, was not modified (Figure 4D). This result indicates that a carboxyl-terminal deletion within Nup159p impairs the stability of the Nup159p/Nsp1p/Nup82p complex but does not interfere with the assembly or stability of the other Nsp1p-containing subcomplex.

Degradation of Nup82Δ108p at 37°C Leads to the Mislocalization of Nup159p

Because affinity purification studies only allow conclusions about whether protein–protein interactions are biochemically stable under specific lysis conditions, and might not accurately reflect the interactions within the living cells, we analyzed the localization of Nup159p, Nup82p, and Nsp1p in the *nup159-1* and

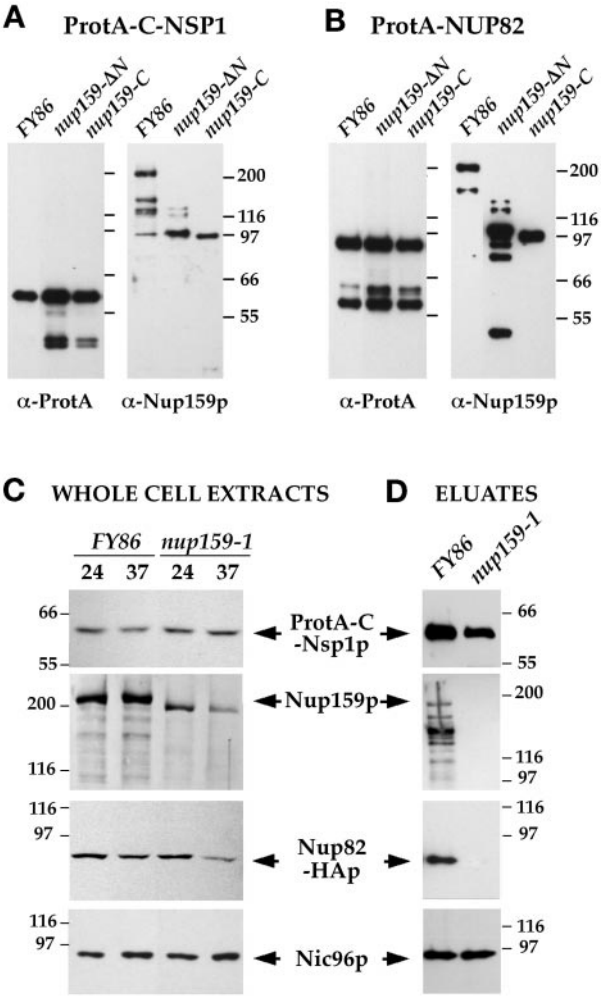

Figure 4. A deletion within the carboxyl-terminal domain of Nup159p impairs the stability of the Nup159p/Nsp1p/Nup82p complex. (A and B) ProtA-C-Nsp1p (A) or ProtA-Nup82p (B), expressed in *FY86* (*NUP159-wt*), a *nup159ΔN*, and a *nup159-C* strain were affinity purified using IgG-Sepharose chromatography, and the affinity-purified fractions were analyzed by Western blotting. IgG coupled to HRP was used to detect the ProtA fusion proteins, whereas the presence of Nup159p was detected using the rat7#5 antibody directed against the carboxyl-terminal domain of Nup159p. Note that full-length Nup159p and Nup159ΔNp proteins were highly sensitive to proteolysis, leading to several breakdown products recognized by the anti-Nup159p antibody, whereas no proteolysis of the Nup159-Cp protein was observed. (C) *FY86* (wt) and *nup159-1* strains, transformed with the pRS316-ProtA-C-NSP1 and pRS314-Nup82-HA plasmids, were grown at 24°C or shifted to 37°C for 3 h. Whole-cell extracts were prepared as described in MATERIALS AND METHODS and analyzed by Western blotting for the presence of ProtA-C-Nsp1p, Nup82-HAp, Nup159p (using the rat7#4 antibody that presents the same affinity for Nup159p and for the truncated Nup159-1p), and Nic96p. After a 3-h shift to 37°C, which induces the degradation of Nup159-1p, the apparent expression level of Nup82-HAp is also decreased. (D) Whole-cell lysates from these two strains grown at 24°C were affinity purified by IgG-Sepharose chromatography. The affinity-purified fractions (eluates) were analyzed by Western blotting and tested for the presence of ProtA-C-Nsp1p, Nup82-HAp, Nup159p, and Nic96p. Unlike wild-type Nup159p, Nup159-1p does not copurify with ProtA-C-Nsp1p. In this mutant strain, the interaction between Nup82-HAp and ProtA-C-Nsp1p was also inhibited, whereas Nic96p still copurified with ProtA-C-Nsp1p.

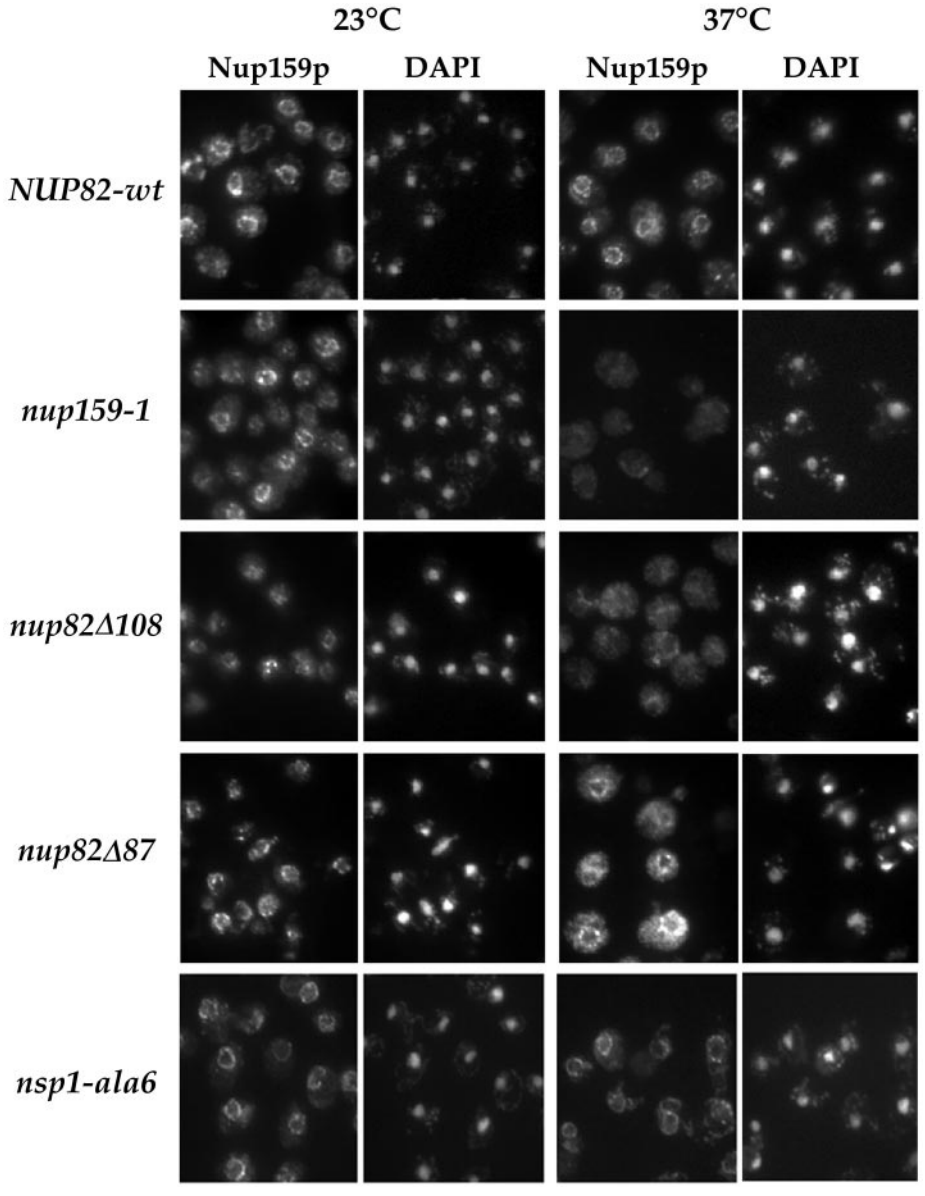

Figure 5. Nup159p is lost from the NPCs when *nup159-1* or *nup82Δ108* cells are shifted to 37°C. Wild-type (*NUP82-wt*), *nup159-1*, *nup82Δ108*, *nup82Δ87*, and *ala6-nsp1* cells were grown at 23°C or shifted for 3 h to 37°C. The subcellular localization of Nup159p was analyzed by immunofluorescence using a polyclonal antibody directed against the repeat-containing domain of Nup159p. Cells were also stained for DNA with DAPI. At 23°C, nuclear pore labeling was observed in all five strains. After a shift to 37°C, a wild-type staining pattern was still observed in the *NUP82-wt*, *nup82Δ87*, and *ala6-nsp1* strains, whereas no perinuclear staining could be detected in the *nup159-1* and *nup82Δ108* strains, indicating that Nup159p had been delocalized from the NPCs in these two strains.

nup82Δ108 mutant strains in which the Nup159-1p and Nup82Δ108p proteins, respectively, are degraded at 37°C.

Immunofluorescence studies, using a specific anti-Nup159p antibody, revealed that in all the strains grown at 23°C, Nup159p was localized at the nuclear periphery (Figure 5). After a 3-h shift to 37°C, Nup159p was still localized at the nuclear rim in the *NUP82-wt*, *nup82Δ87*, and *ala6-nsp1* strains, whereas Nup159p staining was lost from the nuclear periphery in both *nup159-1* and *nup82Δ108* mutant cells. Unlike in the *nup159-1* strain, no specific degradation of Nup159p could be observed in the *nup82Δ108* mutant strain after a 3-h shift to 37°C (see Figure 3B). Accordingly, the lack of nuclear rim staining in the *nup82Δ108* cells grown at 37°C indicates that Nup159p is specifically delocalized from the nuclear pores when Nup82Δ108p is degraded. Even in the *nup82Δ108*

strain at 23°C, there appears to be a reduced amount of Nup159p at the nuclear rim.

Conversely, we analyzed the localization of Nup82p in *nup159-1* cells shifted to 37°C, using a GFP-Nup82p fusion protein. This protein was functional, because it could rescue the otherwise lethal phenotype of an *NUP82*-disrupted strain (our unpublished results). In *NUP82*-disrupted cells, (*NUP159-wt*) GFP-Nup82p gave rise to a typical punctate ring-like staining surrounding the nucleus, although some nonspecific aggregates were occasionally observed in the cytoplasm (Figure 6A). This strain was mated with the *nup159-1* strain, and after sporulation, a *nup159-1* strain expressing GFP-Nup82p as the only form of Nup82p was obtained (strain YV384; see Table 2). In agreement with previous immunofluorescence and electron microscopy studies demonstrating the reversible NPC clustering of the *nup159-1* strain (Gorsch *et al.*, 1995), the GFP-Nup82p chimera localized to the clustered NPCs present in *nup159-1* cells grown at 23°C. After a 3-h shift at 37°C, which induces the degradation of Nup159-1p and a concomitant redistribution of the clustered NPCs (Gorsch *et al.*, 1995), the GFP-Nup82p protein regained a ring-like pattern around the nuclear envelope, indicating that degradation of Nup159-1p at 37°C in the *nup159-1* mutant strain did not lead to a complete delocalization of the GFP-Nup82p protein (Figure 6A). However, the GFP staining within the cytoplasm was somewhat enhanced at 37°C. The same result was obtained in the presence of cycloheximide, indicating that accumulation of GFP in the cytoplasm was not due to a failure to incorporate newly synthesized GFP-Nup82p into NPCs (Snay-Hodge and Cole, unpublished results). Accordingly, this cytoplasmic background could reflect either a partial delocalization of GFP-Nup82p or the degradation of a fraction of this protein. This latter hypothesis being consistent with the apparent degradation of Nup82-HAp independently observed in *nup159-1* cells after a 3-h shift to 37°C (see Figure 4C).

The loss of Nup159p from the NPCs in *nup82Δ108* cells grown at 37°C, together with the persistence of a perinuclear GFP-Nup82p staining in *nup159-1* cells shifted to 37°C, therefore indicates that Nup82p most likely anchors Nup159p at the NPC even though the stabilization of this complex may require the presence of the three proteins. Because our affinity purification studies revealed that in the *nup82Δ108* strain, ProtA-C-Nsp1p stably interacts with Nup159p even at 37°C (Figure 3B), we determined whether a fraction of Nsp1p might be delocalized from the NPCs in *nup82Δ108* and *nup159-1* cells after a 3-h shift to 37°C. Therefore, the in vivo localization of GFP-tagged Nsp1p was analyzed in wild-type, *nup159-1*, and *nup82Δ108* cells (Figure 6B). At 20°C, GFP-C-Nsp1p was localized at NPCs that were homogeneously dis-

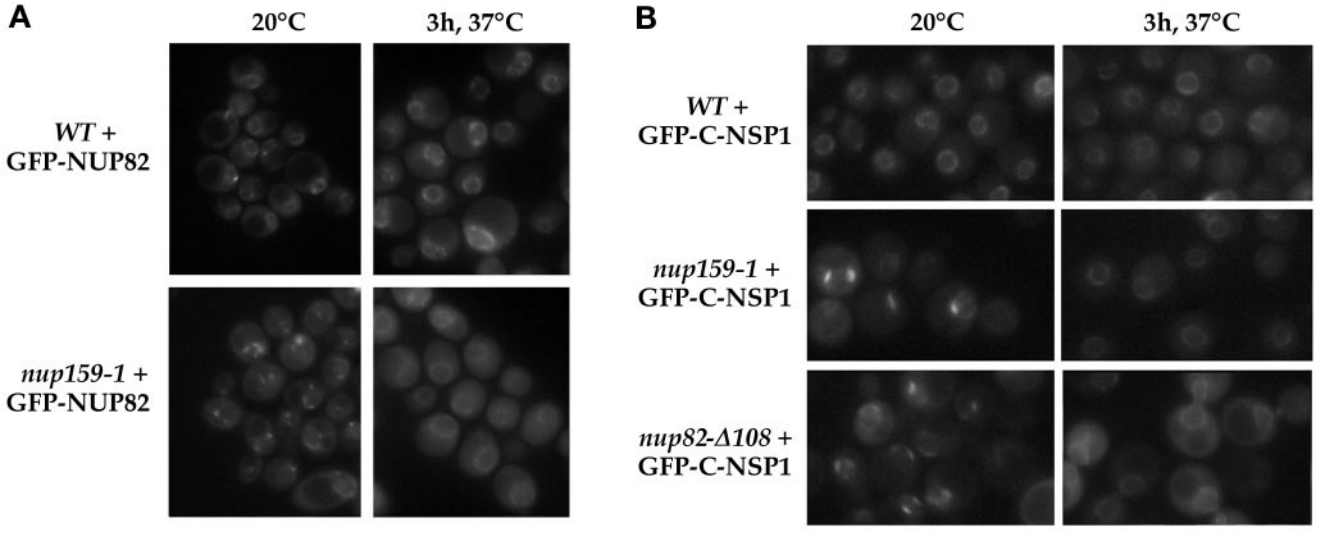

Figure 6. *In vivo* localization of GFP-Nup82p and GFP-Nsp1p in the *nup159-1* or *nup82Δ108* mutant strains. (A) The GFP-NUP82 fusion gene was expressed in a *NUP82*-disrupted strain and in a *nup82::HIS3/nup159-1* strain (strain YV384). The GFP-Nup82p staining was observed by fluorescence microscopy in living cells grown at 20°C or shifted for 3 h to 37°C as described in MATERIALS AND METHODS. In wild-type *NUP159* cells, the GFP-Nup82p fusion protein was localized at the NPCs and gave a ring-like staining at both 20 and 37°C. In *nup159-1* mutant cells grown at 20°C, the GFP-Nup82p was less homogeneously distributed around the nuclear envelope because of the NPC clustering phenotype of the *nup159-1* strain. After a 3-h shift to 37°C that leads to a redistribution of the NPCs, the GFP-Nup82p was still localized at the NPC in the *nup159-1* strain, although enhanced cytoplasmic staining is also evident. (B) The GFP-C-NSP1 construct was introduced in a wild-type (WT) strain and the *nup159-1* and *nup82Δ108* strains. Cells were grown at 20°C or shifted for 3 h at 37°C. In wild-type cells, GFP-Nsp1p gave a ring-like staining at both 20 and 37°C. In *nup159-1* and *nup82Δ108* strains, the GFP-Nsp1p labeling was restricted to a few clusters at 20°C and gave rise to a homogeneous ring staining after a 3-h shift to 37°C.

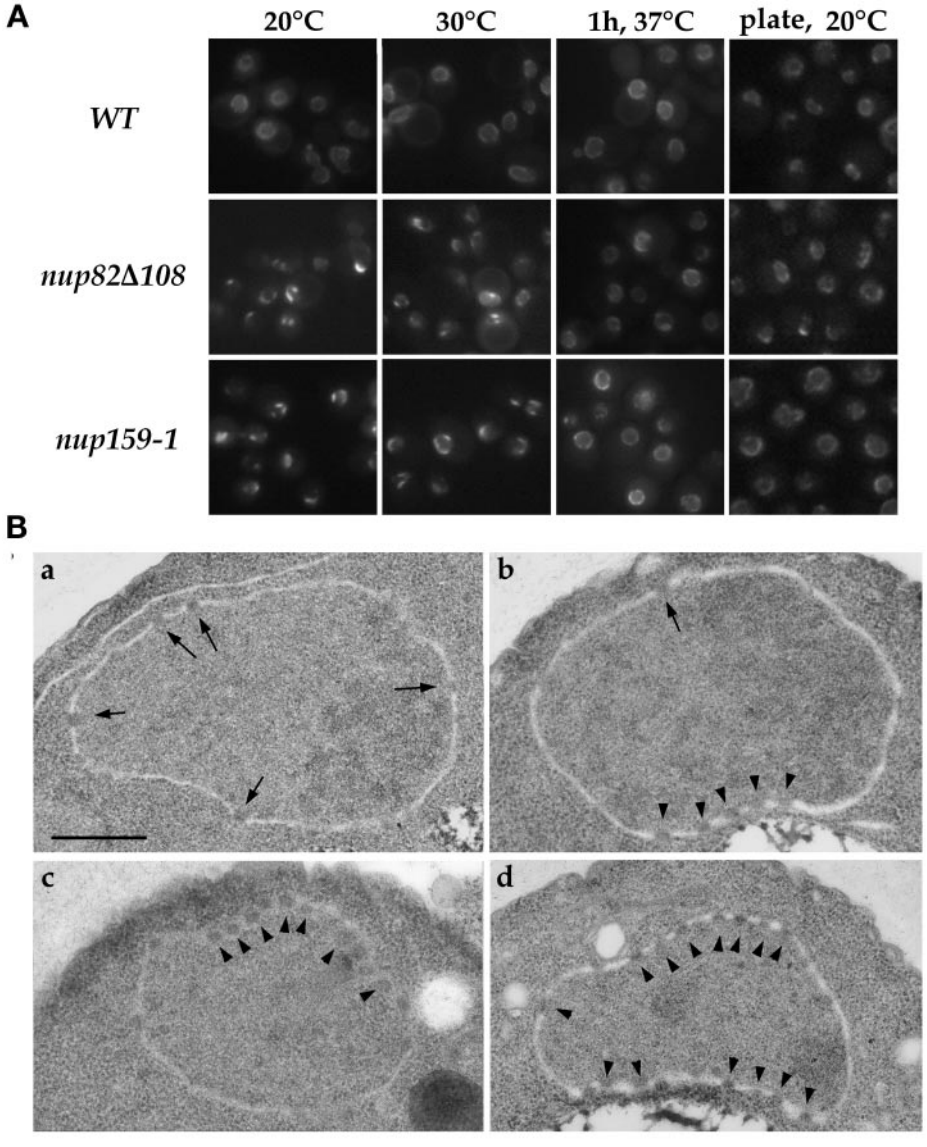

Figure 7. The *nup82Δ108* mutant exhibits a mild and reversible NPC clustering phenotype. (A) To analyze NPC distribution *in vivo*, wild-type (WT), *nup82Δ108*, and *nup159-1* strains were transformed with the pFL38-GFP-NUP49 plasmid. Yeast cells were grown in liquid SD medium lacking uracil to early log phase at 20 or 30°C, grown at 20°C, and shifted for 1 h to 37°C or grown on plates at 20°C for 2 d. These cells were examined for GFP fluorescence as described in MATERIALS AND METHODS. Wild-type cells displayed a homogeneous labeling pattern around the nuclear envelope at all temperatures. In contrast, a mild clustering phenotype was observed in *nup82Δ108* cells and *nup159-1* cells at 20°C and to a lesser extent at 30°C. This clustering phenotype is reversed after a 1-hour shift to 37°C. Strikingly, *nup82Δ108* and *nup159-1* cells grown on plates at 20°C exhibited a homogeneous staining of the nuclear envelope. (B) Electron micrographs of nuclei from wild-type (a) and *nup82Δ108* (b–d) strains grown at 16°C. Wild-type cells have nuclei with evenly distributed NPCs, whereas nup82Δ108 cells exhibited grouped or clustered NPCs. Bar, 0.5 μm. Arrows point to single NPCs, and arrowheads point to clustered nuclear pores.

tributed in the wild-type strain and clustered in the *nup159-1* strain and unexpectedly also in the *nup82Δ108* strain. After a 3-h shift to 37°C, the nuclear envelope was uniformly stained, reflecting redistribution of clustered NPCs. Most of the GFP-C-Nsp1p protein remained at the nuclear envelope in both the wild-type and the two mutant strains, with no significant increase of the cytoplasmic GFP labeling (Figure 6B). Accordingly, if as anticipated, a fraction of GFP-Nsp1p involved in the Nsp1p/Nup82p/Nup159p complex is delocalized from the NPCs, this result indicates that only a minor fraction of Nsp1p is found in this complex compared with the fraction of Nsp1p in the Nsp1p/Nup49p/Nup57p/Nic96p complex (also see DISCUSSION).

Carboxyl-terminal Truncations of Nup159p and Nup82p Lead to Similar Defects in NPC Distribution and Nucleocytoplasmic Transport

To assess the specificity of the clustering phenotype observed with the GFP-C-NSP1 construct in *nup82Δ108* cells grown at 20°C, we introduced the GFP-NUP49 construct (Belgareh and Doye, 1997) into the *nup159-1* and *nup82Δ108* strains and examined the in vivo localization of the GFP-Nup49p chimera at various temperatures. In *nup82Δ108* cells grown to early log phase at temperatures between 16 and 20°C, a mild NPC clustering phenotype, similar to the one observed in *nup159-1* cells, was observed (Figure 7A). However, this clustering phenotype was not as striking as the one observed in other clustering mutants,

such as an *nup133*$^-$ mutant strain (Belgareh and Doye, 1997), because a faint fluorescent signal was still detected around the nuclear envelope. Thin section electron microscopy confirmed this nonhomogeneous NPC distribution and further revealed that this mild clustering phenotype was not associated with major alterations in the structure of the nuclear envelope (Figure 7B). This clustering phenotype was less pronounced when *nup82Δ108* cells were grown at 30°C, and a wild-type distribution of the nuclear pores was restored when cells grown at 20°C were shifted for 1 h to 37°C (Figure 7A). This result thus demonstrates that *nup82Δ108* cells, like *nup159-1* cells, display a reversible clustering of nuclear pores. Interestingly, the ability to analyze NPC distribution in living yeast cells further revealed that *nup159-1* and *nup82Δ108* cells grown on plates, or reaching late log phase in liquid culture, did not display any major defect in nuclear pore distribution (Figure 7A).

Besides this highly reversible alteration in NPC distribution, both *nup159-1* and *nup82Δ108* mutant strains display major defects in poly(A)$^+$ RNA export (Gorsch *et al.*, 1995; Hurwitz and Blobel, 1995). Because a mutation in Crm1p/Xpo1p, a shuttling protein that shows homology to importin β–like transport factors, leads to defects in export of both NES-bearing proteins and poly(A)$^+$ RNA, it was suggested that these pathways might be tightly coupled in *Saccharomyces cerevisiae* (Stade *et al.*, 1997). This result therefore prompted us to investigate nuclear protein export in *nup82Δ108* and *nup159-1* mutant cells expressing the NLS-GFP2-NES fusion protein. Strikingly, although *xpo1-1* mutant cells rapidly accumulated the NLS-GFP2-NES fusion protein inside the nucleus after a shift to 37°C, no major alteration in the localization of NLS-GFP2-NES was detected in the *nup82Δ108* and *nup159-1* cells, even after a shift to 37°C for 3 h. In both cases, only a few cells displayed a modest accumulation of the NLS-GFP2-NES reporter at the nuclear periphery (Figure 8). This stands in contrast to the rapid inhibition of poly(A)$^+$ RNA export that was previously reported in these two mutant strains (Gorsch *et al.*, 1995; Hurwitz and Blobel, 1995) and thus indicates that export of poly(A)$^+$ RNA and NES-bearing proteins can be uncoupled.

In some mutant strains such as *mtr10* or *kap104* knockout strains, inhibition of mRNA export appeared as an indirect consequence of a defect in the import of specific heterogeneous nuclear ribonucleoproteins (hnRNPs) (Aitchison *et al.*, 1996; Senger *et al.*, 1998). We therefore analyzed Npl3p and Nab2p localization in *nup159-1* and *nup82Δ108* cells shifted for 1 h to 37°C (a time point at which, as previously published, poly(A)$^+$ RNA export is greatly inhibited in these strains). Immunofluorescence studies revealed that these two hnRNPs remained entirely nuclear in the *nup159-1* and *nup82Δ108* mutant strains, whereas under the same conditions, Npl3p and

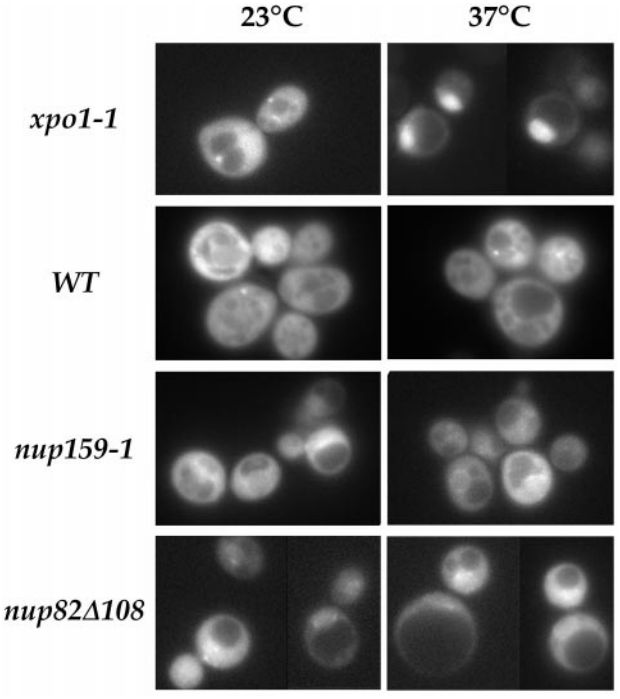

Figure 8. *nup159-1* and *nup82Δ108* cells do not display a major defect in NES-mediated protein export at 37°C. *xpo1-1*, wild-type (FY86), *nup159-1*, and *nup82Δ108* cells were transformed with the NES-GFP2-NLS plasmid. Cells were maintained at 23°C or shifted to 37°C for 3 h. In *xpo1-1* cells shifted to 37°C, an intranuclear accumulation of the NES-GFP2-NLS reporter and a concomitant decrease of the cytoplasmic staining was observed. In contrast, only a slight perinuclear accumulation of the reporter fusion protein could be observed in *nup159-1* and *nup82Δ108* cells shifted to 37°C.

Nab2p were virtually entirely cytoplasmic in *mtr10* and *kap104* knockout strains, respectively (Snay-Hodge and Cole, unpublished results). This demonstrates that unlike in these two karyopherin mutant strains, the defect in poly(A)$^+$ RNA export observed in *nup159-1* and *nup82Δ108* cells is not an indirect consequence of a defect in Npl3p or Nab2p import, even though one cannot exclude that transport of another hnRNP or a specific mRNA transport factor might be inhibited in these strains.

Although *nup159* and *nup82* mutant strains display major defects in poly(A)$^+$ RNA export (Gorsch *et al.*, 1995; Grandi *et al.*, 1995a; Hurwitz and Blobel, 1995; Del Priore *et al.*, 1998), all of the *nsp1* mutant strains so far described were defective mainly for nuclear protein import (Mutvei *et al.*, 1992; Nehrbass *et al.*, 1993). Previous studies using the NLS-β-galactosidase reporter did not allow conclusions as to whether *nup82Δ108* cells were competent for nuclear protein import at the restrictive temperature because the level of expression of the reporter was extremely low, most likely as a consequence of the mRNA export defect (Hurwitz and Blobel, 1995). We therefore reinvestigated nuclear protein import in

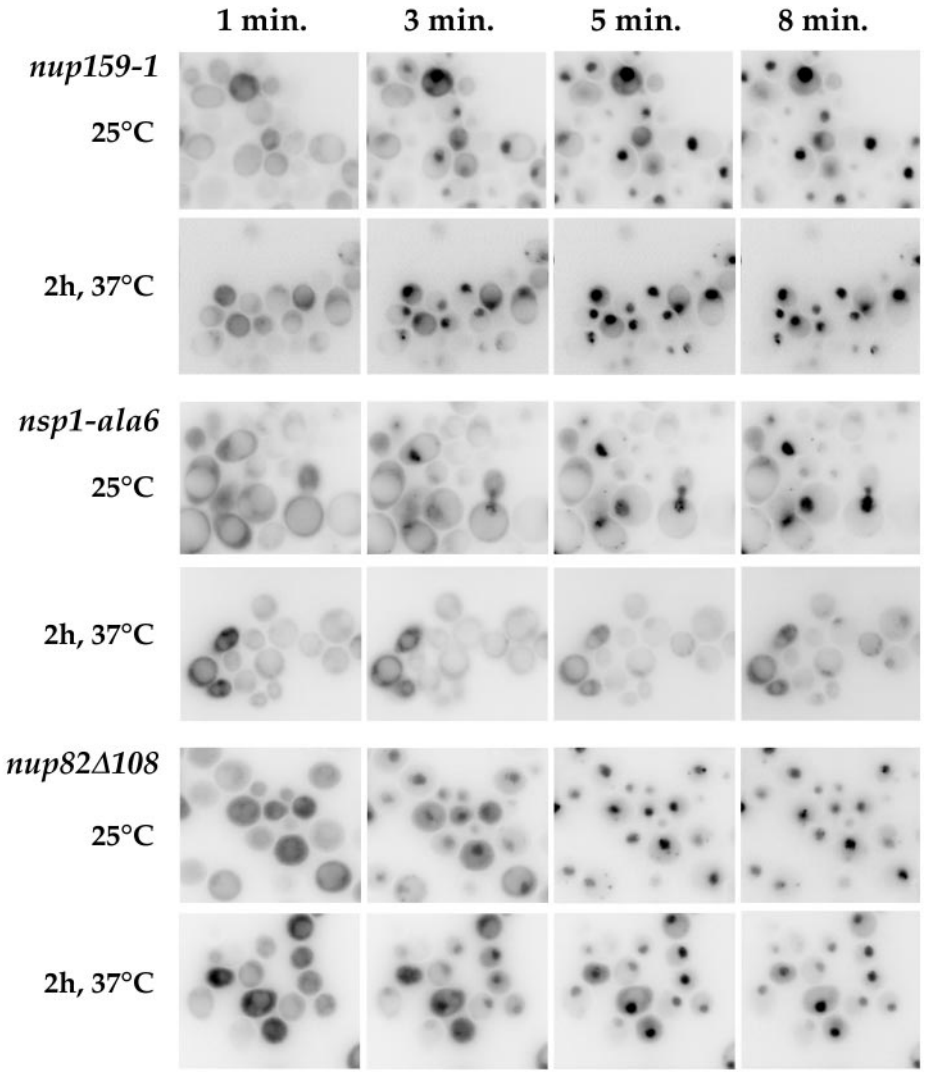

Figure 9. *In vivo* analysis of the nuclear import of Mig1-GFP-lacZ in ts *nup159*, *nsp1*, and *nup82* mutant strains. Temperature-sensitive *nup159, nsp1*, and *nup82* mutant cells expressing the Mig1-GFP-LacZ reporter protein were grown in glycerol-containing medium at the indicated temperatures. At this stage, glucose was added, and living cells were examined and recorded at 1, 3, 5, and 8 min after glucose addition. A rapid nuclear import of the reporter was observed in the *nup159-1* and *nup82Δ108* mutant strains at both 23 and 37°C. In contrast, a modest defect in import was seen in *nsp1-ala6* mutant cells grown at 25°C, and only a few *nsp1-ala6* mutant cells shifted for 2 h to 37°C displayed any import of reporter protein, even 8 min after glucose addition. Note that to improve the detection of the faint nuclear signal, the images have been converted to negative images using the Adobe Photoshop program.

the *nup82Δ108* mutant strain, using the recently characterized Mig1p-GFP-β-galactosidase reporter (De Vit *et al*., 1997). The nuclear import of this reporter can be induced by addition of glucose, which enables one to follow the in vivo import of a nondiffusible protein without any additional cell treatment. As controls, we used the *nup159-1* mutant strain that is not defective for nuclear protein import (Gorsch *et al*., 1995; Del Priore *et al*., 1998) and the ts *nsp1-ala6* mutant strain (Wimmer *et al*., 1992b). In *nup159-1* mutant cells, full nuclear import of the reporter was achieved within 5–8 min after addition of glucose, even when cells had already been shifted to 37°C for 2 h (Figure 9). In contrast, the nuclear import of Mig1p-GFP-β-galactosidase was somewhat defective in *nsp1-ala6* mutant cells grown at permissive temperature and clearly inhibited when these cells were shifted to 37°C for 2 h (Figure 9). At this temperature, only a fraction (~30%) of *nsp1-ala6* cells displayed a faint accumulation of the reporter 10 min after addition of glucose. As shown in Figure 9, *nup82Δ108* mutant cells did not display any major alteration in the rate of import of this reporter, even after a 2-h shift to 37°C, a time at which nuclear export of poly(A)$^+$ RNA is drastically inhibited in this strain (Hurwitz and Blobel, 1995). We conclude

that unlike the *ts nsp1* mutant strains characterized to date, the *nup82Δ108* and *nup159-1* strains have little if any defect in nuclear protein import.

DISCUSSION

In this study the use of protease-deficient strains expressing various protein A-tagged nucleoporins enabled us to demonstrate that Nup159p can be isolated as part of a subcomplex that also contains both Nsp1p and Nup82p. Our data, together with previous studies demonstrating the physical association of a fraction of Nsp1p with Nup82p (Grandi *et al.*, 1995a), indicate that Nsp1p, Nup82p, and Nup159p constitute a nuclear pore subcomplex. The fact that Nup159p had not been detected previously in physical association with Nsp1p or Nup82p (Grandi *et al.*, 1993, 1995a) is most likely due to its sensitivity to proteolysis (Gorsch *et al.*, 1995; Kraemer *et al.*, 1995) and its poor labeling upon silver staining (our unpublished results). Coomassie blue staining of ProtA-Nup82p affinity-purified fractions further indicates that Nup82p belongs to a unique NPC subcomplex. This stands in contrast to Nsp1p, which appears to be part of two NPC subcomplexes (Grandi *et al.*, 1995a). Because immunogold electron microscopy previously located Nup159p at the cytoplasmic side of the nuclear pore complex (Kraemer *et al.*, 1995), the Nup82p/Nsp1p/Nup159p subcomplex itself most likely has the same location. In agreement with this hypothesis, Nup82p has been localized recently by immunogold electron microscopy to the cytoplasmic side of the NPCs (Fahrenkrog *et al.*, 1998; Hurwitz *et al.*, 1998).

Analysis of the interactions among these three nucleoporins in various mutant strains demonstrated that the Nup159p essential carboxyl-terminal domain, previously shown to contain sufficient information for the targeting to NPCs (Del Priore *et al.*, 1998) is essential for its interactions with Nsp1p and Nup82p. In addition, our studies indicate that the carboxyl-terminal domains of Nsp1p and Nup82p, containing heptad repeats, are sufficient for their interaction with Nup159p. Together with previous studies characterizing the interaction between Nsp1p and Nup82p (Grandi *et al.*, 1995a), these results therefore demonstrate that within this NPC subcomplex, interactions are mediated through heptad repeat regions, most likely forming intermolecular coiled coils. Further analysis of the Nsp1p/Nup82p/Nup159p subcomplex using the *nup159-1* mutant strain that produces a protein truncated within its carboxyl-terminal domain revealed that under conditions in which the Nup159-1p mutant protein no longer efficiently interacts with ProtA-C-Nsp1p, the interaction between ProtA-C-Nsp1p and Nup82p was also inhibited. In contrast, a 108-amino acid deletion at the carboxyl terminus of Nup82p prevented its interaction with Nsp1p but did not affect the interaction between Nup159p and Nsp1p. Similarly, it was reported previously that deletions within the heptad repeat domain of Nic96p impair the interaction of Nic96p with the Nsp1p/Nup57p/Nup49p subcomplex (Grandi *et al.*, 1995b). These results therefore suggest a common organization within the Nup82/Nsp1p/Nup159p and Nic96p/Nsp1p/Nup49p/Nup57p subcomplexes, with a heptad repeat containing nucleoporin (respectively Nup82p or Nic96p) acting as a docking site for an NPC subcomplex composed of nucleoporins containing both coiled-coil domains and nucleoporin repeat motifs.

In agreement with this hypothesis, immunofluorescence analysis effectively demonstrated that Nup159p was delocalized from the NPC in *nup82Δ108* cells shifted to 37°C, a temperature at which the Nup82Δ108p mutant protein becomes degraded. In addition, affinity purification studies demonstrating that Nsp1p and Nup159p are stably associated in the *nup82Δ108* strain even at 37°C suggest that Nup82p might anchor both Nup159p and Nsp1p at the NPC. However, in vivo analysis of GFP-C-Nsp1p localization in the *nup82Δ108* mutant cells did not allow the identification of a major cytosolic fraction of Nsp1p delocalized at 37°C. Because Nsp1p is part of two distinct subcomplexes, the most likely explanation is that only a minor, not clearly detectable fraction of Nsp1p is associated with Nup82p and Nup159p. Even though this study does not allow precise quantitation of this fraction, the fact that a minor fraction of Nsp1p is engaged in the Nsp1p/Nup159p/Nup82p complex is in agreement with the reproducible lower fraction of Nsp1p that could be copurified with ProtA-Nup82p compared with the fraction that copurified with ProtA-Nup49p (Figure 1B, compare the amount of Nsp1p detected by Coomassie blue staining and by Western blotting using an anti-Nsp1p antibody).

All the ts mutants of *NSP1* analyzed so far (including the *nsp1-ala6* allele) map within the first heptad repeat region of its carboxyl-terminal domain, a region required for complex formation with Nup49p and Nup57p (Wimmer *et al.*, 1992a; Nehrbass *et al.*, 1993; Schlaich *et al.*, 1997). Our biochemical and fluorescence data, demonstrating that the interaction between Nsp1-ala6p and both Nic96p and Nup82p is similarly compromised in the presence of competing wild-type Nsp1p, suggest that identical or overlapping domains within the heptad-repeat sequence of Nsp1p might be involved in interactions with both the Nsp1p/Nup159p/Nup82p and the Nsp1p/Nup49p/Nup57p/Nic96p NPC subcomplexes. Because all of the characterized mutants of *NSP1* display major defects in nuclear protein import (Mutvei *et al.*, 1992; Nehrbass *et al.*, 1993), we therefore examined whether the *nup82Δ108* mutant, which may alter the localization of a fraction of Nsp1p, would also be defective for nuclear protein import. However, in vivo analyses of nuclear protein import, using Mig1-GFP-β-galactosidase as a reporter, although confirming and extending to this reporter the role of Nsp1p in nuclear protein import (Mutvei *et al.*, 1992; Nehrbass *et al.*, 1993), did not

reveal any nuclear protein import defect in the *nup82Δ108* mutant strain at times at which nuclear export of poly(A)$^+$ RNA is drastically inhibited. This stands in contrast to the defect in the rate of nuclear import of an SV40-NLS-GFP fusion protein that has been previously reported for the ts *nup82-3* mutant allele (Shulga *et al.*, 1996). Although one cannot exclude that *nup82* mutant cells might have an import rate defect for the SV40-NLS substrate but not for Mig1p, a pleiotropic defect of the *nup82-3* mutant allele, which has so far not been further characterized, cannot be excluded. One can thus speculate that the fraction of Nsp1p that associates with Nup82p and Nup159p on the cytosolic face of the NPC is not required for proper nuclear protein import. This fraction of Nsp1p could thus either perform a nonessential function or be involved in other transport processes.

Although the function of Nsp1p within the Nsp1p/Nup159p/Nup82p NPC subcomplex remains to be clarified, the *nup159-1* and *nup82Δ108* mutant strains display very similar phenotypes. In both cases, a deletion within the carboxyl-terminal domain of these proteins leads to a major defect in poly(A)$^+$ RNA export at 37°C, suggesting that the defect in poly(A)$^+$ RNA export observed in the *nup82Δ108* strain could be due to the loss from NPCs of the repeat-containing nucleoporin Nup159p. However, as discussed by Ohno *et al.* (1998), this apparent specific defect in poly(A)$^+$ RNA export may reflect a structural defect, serious enough to prevent export of large hnRNP particles but not import or export of smaller transport substrates. In addition to this transport defect that occurs at restrictive temperature, the *nup159-1* and *nup82Δ108* mutant strains both display a mild and highly reversible clustering of the NPCs. In particular, this clustering phenotype appeared to depend on the growth conditions, because *nup159-1* or *nup82Δ108* cells from dense liquid culture or grown on plates showed a normal NPC distribution. Whether this redistribution could be somehow linked to the induction of specific stress response genes that can be turned on under such growth conditions remains to be determined. Moreover, this particular phenotype gives a specificity to the essential Nup159p and Nup82p nucleoporins, which seem to have a different role in NPC distribution than the nonessential components of the Nup84p/Nup85p/Nup120p/C-Nup145p subcomplex, whose deletion individually led to a constitutive clustering of the NPCs associated with structural alterations of the nuclear envelope (Wente and Blobel, 1994; Aitchison *et al.*, 1995a; Heath *et al.*, 1995; Goldstein *et al.*, 1996; Siniossoglou *et al.*, 1996; Teixeira *et al.*, 1997).

Although the overall structure of the nuclear pore and its functions have been conserved from yeast to vertebrates, few yeast nucleoporins show a very high degree of homology to any metazoan nucleoporins over their entire length. In addition, in only one case has it been possible to substitute a metazoan nucleoporin for a yeast nucleoporin (Aitchison *et al.*, 1995b). Therefore, it is not yet possible to determine directly whether yeast and metazoan nucleoporins that share sequence homology perform homologous roles. However, evidence is beginning to accumulate that suggests that the organization of nucleoporins into functional subcomplexes and, at a higher level, the organization of subcomplexes within NPCs may well be conserved. For instance, p62, which is considered the vertebrate homologue of yeast Nsp1p, has been shown to be associated with p58 and p54 (Finlay *et al.*, 1991; Guan *et al.*, 1995; Hu *et al.*, 1996), which are related to (and may also be homologues of) Nup57p and Nup49p, respectively (Hu *et al.*, 1996; Doye and Hurt, 1997; Schlaich *et al.*, 1997). In addition, a fraction of Nup93, a probable vertebrate homologue of yeast Nic96p, physically interacts with p62, just as yeast Nic96p interacts with Nsp1p (Grandi *et al.*, 1997). Interestingly, yeast Nup159p and vertebrate Nup214/CAN share a similar location on the cytoplasmic side of the NPCs and closely related degenerate FG repeat motifs (Kraemer *et al.*, 1994, 1995). In addition, both Nup159p and Nup214/CAN contain a coiled-coil domain (located respectively within the carboxyl-terminal part of Nup159p and within the central region of Nup214/CAN) that has been shown to be necessary and sufficient for their nuclear pore association (Fornerod *et al.*, 1995; Del Priore *et al.*, 1998). Recently, Nup214/CAN has been shown to associate through its coil-coiled domain with a novel nuclear pore protein referred to as Nup88 or Nup84 (Bastos *et al.*, 1997; Fornerod *et al.*, 1997). Although the sequence homology between Nup88/Nup84 and Nup82p is marginal (Fornerod *et al.*, 1996), Nup88/Nup84, like yeast Nup82p, contains a carboxyl-terminal coiled-coil domain (Bastos *et al.*, 1997; Fornerod *et al.*, 1997). These data suggest that the yeast Nup82p/Nup159p and mammalian Nup88/Nup214 associations could be functionally homologous.

In yeast, a fraction of Nsp1p coprecipitates with Nup159p and Nup82p. Similarly, a minor fraction of *Xenopus* p62 was found in association with a p200 *N*-acetylglucosaminylated protein, the putative *Xenopus* homologue of mammalian Nup214/CAN (Macaulay *et al.*, 1995). Furthermore, a protein of 66 kDa (referred to as CC66) coprecipitates, although less consistently than Nup88, with the coiled domain of Nup214/CAN in mammalian cells (Fornerod *et al.*, 1996). Although the difference in molecular masses is significant, the fact that CC66 could be identical to p62 has not been clearly excluded, leaving open the possibility that a fraction of p62 could interact with the Nup214/Nup88 subcomplex in mammalian cells. If this is the case, the fact that p62 was found to be located on both sides of the NPC at or near the ends of the central plug (Guan *et al.*, 1995) might reflect the low abundance of the fraction of p62 associated with

Nup214 in *Xenopus* (Macaulay *et al.*, 1995). Finally, hCRM1 was found to be associated with CAN/Nup214 (Fornerod *et al.*, 1997). Our preliminary data from two-hybrid analyses suggest that Crm1p/Xpo1p associates with Nup159p (Stafford and Cole, personal communication), extending the similarity between yeast and metazoan cells. However, Crm1p/Xpo1p must associate with other nucleoporins as well, because protein export is maintained in cells in which Nup159p has been lost from nuclear pore complexes.

ACKNOWLEDGMENTS

We thank Michael Hurwitz (Rockefeller University, New York, NY), Ed Hurt (University of Heidelberg, Heidelberg, Germany), Michael De Vit (Washington University School of Medicine, St. Louis, MO), and Karsten Weis (University of California, San Francisco, CA) for plasmids, yeast strains, and antibodies. We thank Michael Hurwitz, Günter Blobel and Nelly Panté for communicating results on the localization of Nup82p before publication. We also thank Michel Bornens (Institut Curie, Paris, France) for constant support, Paola Grandi (Institut Curie), Emmanuelle Fabre, and Ulf Nehrbass (Institut Pasteur, Paris, France) for critical reading of the manuscript and the members of our laboratories for helpful discussions and advice. This work was supported by a Centre National de la Recherche Scientifique grant (UMR144), the Institut Curie, and a grant from the Association pour la Recherche contre le Cancer (all to V.D.) and by grant GM33998 from the National Institute of General Medical Sciences, National Institutes of Health (to C.N.C.). N.B. received a fellowship from the Ministère de l'Enseignement et de la Recherche Supérieure. S.D. was supported by National Research Service Award fellowship AR07576 from the National Institute of Arthirtis and Musculoskeletal Diseases, National Institutes of Health.

REFERENCES

Aitchison, J.D., Blobel, G., and Rout, M.P. (1995a). Nup120: a yeast nucleoporin required for NPC distribution and mRNA export. J. Cell Biol. *131*, 1659–1675.

Aitchison, J.D., Blobel, G., and Rout. M.P. (1996). Kap104p: a karyopherin involved in the nuclear transport of messenger RNA binding proteins. Science *274*, 624–627.

Aitchison, J.D., Rout, M.P., Marelli, M., Blobel, G., and Wozniak, R.W. (1995b). Two novel related yeast nucleoporins Nup170p and Nup157p: complementation with the vertebrate homologue Nup155p and functional interactions with the yeast nuclear pore-membrane protein Pom152p. J. Cell Biol. *131*, 1133–1148.

Aris, J.P., and Blobel, G. (1988). Identification and characterization of a yeast nucleolar protein that is similar to a rat liver nucleolar protein. J. Cell Biol. *107*, 17–31.

Bastos, R., Ribas de Pouplana, L., Enarson, M., Bodoor, K., and Burke, B. (1997). Nup84, a novel nucleoporin that is associated with CAN/Nup214 on the cytoplasmic face of the nuclear pore complex. J. Cell Biol. *137*, 989–1000.

Belgareh, N., and Doye, V. (1997). Dynamics of nuclear pore distribution in nucleoporin mutant yeast cells. J. Cell Biol. *136*, 747–759.

Berges, T., Petfalski, E., Tollervey, D., and Hurt, E.C. (1994). Synthetic lethality with fibrillarin identifies NOP77p, a nucleolar protein required for pre-rRNA processing and modification. EMBO J. *13*, 3136–3148.

Bradford, M.M. (1976). A rapid and sensitive method for the quantitation of microgram quantities of protein utilizing the principle of protein-dye binding. Anal. Biochem. *72*, 248–254.

Byers, B., and Goetsch, L. (1975). Behaviour of spindles and spindle plaques in the cell cycle and conjugation of *Saccharomyces cerevisiae*. J. Bacteriol. *124*, 511–523.

Corbett, A.H., and Silver, P.A. (1997). Nucleocytoplasmic transport of macromolecules. Microbiol. Mol. Biol. Rev. *61*, 193–211.

Cordes, V.V., Reidenbach, S., Rackwitz, H.R., and Franke, W.W. (1997). Identification of protein p270/Tpr as a constitutive component of the nuclear pore complex-attached intranuclear filaments. J. Cell Biol. *136*, 515–529.

De Vit, M.J., Waddle, J.A., and Johnston, M. (1997). Regulated nuclear translocation of the Mig1 glucose repressor. Mol. Biol. Cell *8*, 1603–1618.

Del Priore, V., Heath, C.V., Snay, C.A., MacMillan, A., Gorsch, L.C., Dagher, S., and Cole, C.N. (1998). A structure/function analysis of the Rat7p/Nup159p, an essential nucleoporin of *Saccharomyces cerevisiae*. J. Cell Sci. *110*, 2987–2999.

Doye, V., and Hurt, E. (1997). From nucleoporins to nuclear pore complexes. Curr. Opin. Cell Biol. *9*, 401–411.

Fahrenkrog, B., Hurt, E.C., Aebi, U., and Panté, N. (1998). Molecular architecture of the yeast nuclear pore complex: localization of Nsp1p subcomplexes. J. Cell Biol. (*in press*).

Finlay, D.R., Meier, E., Bradley, P., Horecka, J., and Forbes, D.J. (1991). A complex of nuclear pore proteins required for pore function. J. Cell Biol. *114*, 169–183.

Fornerod, M., Boer, J., Vanbaal, S., Jaegle, M., Vonlindern, M., Murti, K.G., Davis, D., Bonten, J., Buijs, A., and Grosveld, G. (1995). Relocation of the carboxyterminal part of CAN from the nuclear envelope to the nucleus as a result of leukemia-specific chromosome rearrangements. Oncogene *10*, 1739–1748.

Fornerod, M., Boer, J., van Baal, S., Morreau, H., and Grosveld, G. (1996). Interaction of cellular proteins with the leukemia specific fusion proteins DEK-CAN and SET-CAN and their normal counterpart, the nucleoporin CAN. Oncogene *13*, 1801–1808.

Fornerod, M., van Deursen, J., van Baal, S., Reynolds, A., Davis, D., Gopal Murti, K., Fransen, J., and Grosveld, G. (1997). The human homologue of yeast CRM1 is in a dynamic subcomplex with CAN/Nup214 and a novel nuclear pore component Nup88. EMBO J. *16*, 807–816.

Goldstein, A.L., Snay, C.A., Heath, C.V., and Cole, C.N. (1996). Pleiotropic nuclear defects associated with a conditional allele of the novel nucleoporin Rat9p/Nup85p. Mol. Biol. Cell *7*, 917–934.

Gorsch, L.C., Dockendorff, T.C., and Cole, C.N. (1995). A conditional allele of the novel repeat-containing yeast nucleoporin RAT7/NUP159 causes both rapid cessation of mRNA export and reversible clustering of nuclear pore complexes. J. Cell Biol. *129*, 939–955.

Grandi, P., Dang, T., Pane, N., Shevchenko, A., Mann, M., Forbes, D., and Hurt, E. (1997). Nup93, a vertebrate homologue of yeast Nic96p, forms a complex with a novel 205-kDa protein and is required for correct nuclear pore assembly. Mol. Biol. Cell *8*, 2017–2038.

Grandi, P., Doye, V., and Hurt, E.C. (1993). Purification of NSP1 reveals complex formation with "GLFG" nucleoporins and a novel nuclear pore protein NIC96. EMBO J. *12*, 3061–3071.

Grandi, P., Emig, S., Weise, C., Hucho, F., Pohl, T., and Hurt, E.C. (1995a). A novel nuclear pore protein Nup82p which specifically binds to a fraction of Nsp1p. J. Cell Biol. *130*, 1263–1273.

Grandi, P., Schlaich, N., Tekotte, H., and Hurt, E.C. (1995b). Functional interaction of Nic96p with a core nucleoporin complex consisting of Nsp1p, Nup49p and a novel protein Nup57p. EMBO J. *14*, 76–87.

Guan, T., Muller, S., Klier, G., Panté, N., Blevitt, J.M., Haner, M., Paschal, B., Aebi, U., and Gerace, L. (1995). Structural analysis of the p62 complex, an assembly of O-linked glycoproteins that localizes

near the central gated channel of the nuclear pore complex. Mol. Biol. Cell *6*, 1591–1603.

Heath, C.V., Copeland, C.S., Amberg, D.C., Del Priore, V., Snyder, M., and Cole, C.N. (1995). Nuclear pore complex clustering and nuclear accumulation of poly(A)$^+$ RNA associated with mutation of the *Saccharomyces cerevisiae* RAT2/NUP120 gene. J. Cell Biol. *131*, 1677–1697.

Hu, T., Guan, T., and Gerace, L. (1996). Molecular and functional characterization of the p62 complex, an assembly of nuclear pore complex glycoproteins. J. Cell Biol. *134*, 589–601.

Hurwitz, M.E., and Blobel, G. (1995). NUP82 is an essential yeast nucleoporin required for poly(A)$^+$ RNA export. J. Cell Biol. *130*, 1275–1281.

Hurwitz, M.E., Strambio-de-Castillia, C., and Blobel, G. (1998). Two yeast nuclear pore complex proteins involved in mRNA export form a cytoplasmically oriented subcomplex. Proc. Natl. Acad. Sci. USA 95, 11241–11245.

Iovine, M.K., and Wente, S.R. (1997). A nuclear export signal in Kap95p is required for both recycling the import factor and interaction with the nucleoporin GLFG repeat regions of Nup116p and Nup100p. J. Cell Biol. *137*, 797–811.

Kahana, J.A., and Silver, P. (1996). Use of *A. victoria* green fluorescent protein to study protein dynamics in vivo. In: Current Protocols in Molecular Biology, vol. 34, unit 9.7, ed. F.M. Ausubel, R. Brent, R.E. Kingston, D.D. Moore, J.G. Seidman, J.A. Smith, and K. Struhl, Brooklyn, NY: Greene Publishing Associates/Wiley-Interscience, 9.7.22–9.7.28.

Kraemer, D.M., Strambio-de-Castillia, C., Blobel, G., and Rout, M.P. (1995). The essential yeast nucleoporin NUP159 is located on the cytoplasmic side of the nuclear pore complex and serves in karyopherin-mediated binding of transport substrate. J. Biol. Chem. *270*, 19017–19021.

Kraemer, D., Wozniak, R.W., Blobel, G., and Radu, A. (1994). The human CAN protein, a putative oncogene product associated with myeloid leukemogenesis, is a nuclear pore complex protein that faces the cytoplasm. Proc. Natl. Acad. Sci. USA *91*, 1519–1523.

Macaulay, C., Meier, E., and Forbes, D.J. (1995). Differential mitotic phosphorylation of proteins of the nuclear pore complex. J. Biol. Chem. *270*, 254–262.

Maniatis, T., Fritsch, E.T., and Sambrook, J. (1982). Molecular Cloning: A Laboratory Manual, Cold Spring Harbor, NY: Cold Spring Harbor Laboratory Press.

Matunis, M.J., and Blobel, G. (1996). Biochemical and molecular analysis of the mammalian nuclear pore complex and the regulation of nuclear transport. Mol. Biol. Cell *7*, 95a (abstract).

Mutvei, A., Dihlmann, S., Herth, W., and Hurt, E.C. (1992). NSP1 depletion in yeast affects nuclear pore formation and nuclear accumulation. Eur. J. Cell Biol, *59*, 280–295.

Nehrbass, U., Fabre, E., Dihlmann, S., Herth, W., and Hurt, E.C. (1993). Analysis of nucleo-cytoplasmic transport in a thermosensitive mutant of the nuclear pore protein NSP1. Eur. J. Cell Biol. *62*, 1–12.

Nehrbass, U., Kern, H., Mutvei, A., Horstmann, H., Marshallsay, B., and Hurt, E.C. (1990). NSP1: a yeast nuclear envelope protein localized at the nuclear pores exerts its essential function by its carboxy-terminal domain. Cell *61*, 979–989.

Nehrbass, U., Rout, M.P., Maguire, S., Blobel, G., and Wozniak, R.W. (1996). The yeast nucleoporin Nup188p interacts genetically and physically with the core structures of the nuclear pore complex. J. Cell Biol. *133*, 1153–1162.

Neville, M., Stutz, F., Lee, L., Davis, L.I., and Rosbash. M. (1997). The importin-beta family member Crm1p bridges the interaction between Rev and the nuclear pore complex during nuclear export. Curr. Biol. *7*, 767–775.

Nigg, E.A. (1997). Nucleocytoplasmic transport: signals, mechanisms and regulation. Nature *386*, 779–787.

Ohno, M., Fornerod, M., and Mattaj, I.W. (1998). Nucleocytoplasmic transport: the last 200 nanometers. Cell *92*, 327–336.

Panté, N., and Aebi, U. (1996). Toward the molecular dissection of protein import into the nucleus. Curr. Opin. Cell Biol. *8*, 397–406.

Pemberton, L., Rosenblum, J.S., and Blobel, G. (1997). A distinct and parallel pathway for the nuclear import of an mRNA-binding protein. J. Cell Biol. *139*, 1645–1653.

Rosenblum, J.S., Pemberton, L., and Blobel, G. (1997). A nuclear import pathway for a protein involved in tRNA maturation. J. Cell Biol. *139*, 1655–1661.

Rout, M.P., and Blobel, G. (1993). Isolation of the yeast nuclear pore complex. J. Cell Biol. *123*, 771–783.

Schlaich, N.L., Häner, M., Lustig, A., Aebi, U., and Hurt, E.C. (1997). In vitro reconstitution of a heterotrimeric nucleoporin complex consisting of recombinant Nsp1p, Nup49p and Nup57p. Mol. Biol. Cell *8*, 33–46.

Senger, B., Simos, G., Bischoff, F.R., Podtelejnikov, A., Mann, M., and Hurt, E. (1998). Mtr10p functions as a nuclear import receptor for the mRNA- binding protein Np13p. EMBO J. *17*, 2196–2207.

Shulga, N., Roberts, P., Gu, Z., Spitz, L., Tabb, M.M., Nomura, M., and Goldfarb, D.S. (1996). In vivo nuclear transport kinetics in *Saccharomyces cerevisiae*: a role for heat shock protein 70 during targeting and translocation. J. Cell Biol. *135*, 329–339.

Sikorski, R.S., and Hieter, R. (1989). A system of shuttle vectors and yeast host strains designed for efficient manipulation of DNA in *Saccharomyces cerevisiae*. Genetics *122*, 19–27.

Siniossoglou, S., Wimmer, C., Rieger, M., Doye, V., Tekotte, H., Weise, C., Emig, S., Segref, A., and Hurt, E.C. (1996). A novel complex of nucleoporins, which includes Sec13p and a Sec13p homolog, is essential for normal nuclear pores. Cell *84*, 265–275.

Stade, K., Ford, C.S., Guthrie, C., and Weis, K. (1997). Exportin 1 (Crm1p) is an essential nuclear export factor. Cell *90*, 1041–1050.

Teixeira, M.T., Siniossoglou, S., Podtelejnikov, S., Benichou, J.C., Mann, M., Dujon, B., Hurt, E., and Fabre, E. (1997). Two functionally distinct domains generated by in vivo cleavage of Nup145p: a novel biogenesis pathway for nucleoporins. EMBO J. *16*, 5086–5097.

Wente, S.R., and Blobel, G. (1994). NUP145 encodes a novel yeast glycine-leucine-phenylalanine-glycine (GLFG) nucleoporin required for nuclear envelope structure. J. Cell Biol. *125*, 955–969.

Wente, S.R., Gasser, S.M., and Caplan, A.J. (1996). The nucleus and nucleocytoplasmic transport in Saccharomyces cerevisiae. In: The Molecular and Cellular Biology of the Yeast *Saccharomyces*, vol. 3, ed. J.R. Broach, E. Jones, and J. Pringle, Cold Spring Harbor, NY: Cold Spring Harbor Laboratory Press, 471–542.

Wimmer, C., Doye, V., Grandi, P., Nehrbass, U., and Hurt, E. (1992a). A new subclass of nucleoporins that functionally interacts with nuclear pore protein NSP1. EMBO J. *11*, 5051–5061.

Wimmer, C., Doye, V., Nehrbass, U., Schlaich, N., and Hurt, E.C. (1992b). Approaches towards a genetic analysis of the nuclear pore complex in yeast. In: Protein Synthesis and Targeting in Yeast, NATO ASI series H, vol. 71, ed. A.J.P. Brown, M.F. Tuite, and J.E.G. McCarthy. Berlin: Springer-Verlag, 269–281.

Wright, R., and Rine, J. (1989). Transmission electron microscopy and immunocytochemical studies of yeast: analysis of HMG-CoA reductase overproduction by electron microscopy. Methods Cell Biol. *31*, 473–512.

Yaseen, N.R., and Blobel, G. (1997). Cloning and characterization of human karyopherin beta 3. Proc. Natl. Acad. Sci. USA *94*, 4451–4456.